DESIGN OF BUILDINGS THROUGH LINEAR TIME-HISTORY ANALYSIS OPTIMISING GROUND MOTION SELECTION: A CASE STUDY FOR RC-MRF

Luca Lombardi[1], Flavia De Luca[1], and John Macdonald[1]

[1]Department of Civil Engineering, University of Bristol, Bristol, United Kingdom

A novel framework for Eurocode 8-compliant design using Linear Time-History Analysis (LTHA) is discussed. LTHA overcomes the approximations typical of other linear seismic analyses but it still lacks a suitable approach for seismic input selection compatible with Eurocode 8-prescriptions. The critical aspect is to find a balanced compromise to control seismic input variability, suiting design purposes, but still being able to capture specific response features such as pulse-like effects. A LTHA design procedure has been included in ASCE/SEI 7-16 (2017) and described in FEMA P-1050 (2015), suggesting spectral-matching of three ground motions as input, so that LTHA can be used as alternative to Response Spectrum Analysis (RSA). Herein, a 12-storey regular Reinforced Concrete Moment Resisting Frame building is employed as case-study. Different ground motion selection strategies are compared. Firstly, three suites of spectrum-compatible ground motions are used referring to requirements of Eurocode 8 for nonlinear time-history analysis and compared with LTHA-ground motion selection procedure included in FEMA P-1050.
A new index for LTHA ground motion selection (I_{eq}) is proposed to control response variability in relation to the dynamic properties of the structure aimed at obtaining a suitable input for LTHA design. A target value for I_{eq} is proposed on the basis of structural response for far-field and near-field suites and an *ad hoc* suite of pulse-like ground motions selected considering pulse periods lower than the fundamental period of the structure. The difference in terms of design results between LTHA and RSA is employed as benchmark to evaluate the suitability of I_{eq} for LTHA design.

KEYWORDS

Linear Time-History Analysis; Eurocode 8; Far-Field; Near-Field; Ground Motion Selection; Pulse-like.

1. INTRODUCTION

The routine analysis approach for code-based seismic design of buildings is generally linear and it accounts for ductility and nonlinear behaviour in an approximate way through the so-called “behaviour factor” (denoted by *q*) in Eurocode 8 (EC8, CEN 2004a [1]) or “strength reduction factor” (denoted by *R*) in United States standards (e.g., ASCE/SEI 7-16, ASCE 2017 [2]). The *q* factor is used for design purposes to reduce the elastic response spectrum for linear analyses. It accounts for the nonlinear response of a structure, associated with the material, the structural system and the design procedures (e.g., Mwafi and Elnashai 2002 [3]). All design approaches using *q* to reduce seismic forces are called “force-based” approaches. Among such methods, the Lateral Force Method (LFM) assumes a predefined force distribution (based on the mass distribution) and it is allowed for first-mode dominated buildings, regular in plan and elevation, with a fundamental period within specific ranges defined by codes.
Many standards and codes, including EC8, assume modal Response Spectrum Analysis (RSA) as the reference method for design. RSA is an approximate approach for evaluating the linear dynamic response of buildings (e.g., Chopra 2012 [4]). Its approximation, well-known since the 1980s, is in the combination of contributions from multiple modes. The Complete Quadratic Combination (CQC) is the most accurate combination rule for RSA for its applicability to a wide class of structures, as suggested in many codes and standards such as EC8, NZS 1170.5 (SNZ 2004 [5]), NTC (Italian Building Code 2018 [6]), and ASCE/SEI 7-16. However, the CQC presents some limitations for near-source impulsive earthquakes, unusually stiff buildings (such as dams or nuclear power plants) and higher mode dominated buildings, as discussed by many authors (e.g., Der Kiureghian 1981 [7]; Gupta 1992 [8]; Cacciola et al. 2004 [9]; De Luca and Verderame 2013 [10]; among others). Another weakness of RSA is that the combination of modal effects does not capture the sign and coupling of different components of member actions and system deformations. For example, it becomes an issue when the maximum Demand/Capacity (*D/C*) ratio of a

structural member subjected to the combined action of axial force and bending moment over time, for all load combinations, needs to be evaluated (e.g., Wilson 2015 [11]; Charney 2015 [12]).

As a result of the widespread use of RSA, current professional practice in design still needs refinements; a balanced compromise between accuracy of structural response evaluation and simplicity of design procedure for all possible practical cases (i.e., high-rise, low-rise, regular and irregular structures) should be the target. For this reason, Linear Time-History Analysis (LTHA), also known as Linear Response-History Analysis (LRHA), represents an appealing alternative to overcome the approximate assumptions typical of linear analyses (i.e., preassigned distribution of lateral forces, loss of both sign and coupling of local force components when modal combination rules are used, etc.), but also a simple tool for design (Charney 2015 [12]; De Luca and Lombardi 2017 [13]). Furthermore, LTHA can reliably estimate the behaviour of buildings in serviceability conditions (i.e., when behaviour is essentially elastic and limited structural damage is expected). This is an important aspect, since experience has shown that a relevant part of economic losses due to medium or severe earthquakes is attributed to non-structural damage, especially for commercial, industrial and strategic buildings (e.g., Taghavi and Miranda 2003 [14]). LTHA, indeed, allows engineers to determine other response quantities as well, such as absolute accelerations, relative accelerations and velocities, since some equipment can be sensitive to these response quantities. Having a reliable estimation of serviceability performance at the design stage can be very valuable for decision making. In fact, engineers have already been using LTHA for *ad hoc* analyses in advanced applications (such as bridges, dams, nuclear facilities, etc., Ghanaat 2004 [15]; Yamaguchi et al. 2004 [16]; Nour et al. 2012 [17]). Therefore, the proposal of a validated code-based LTHA design framework for buildings, which can be implemented in EC8, represents an important opportunity for engineers.

Generally, LTHA results in higher structural response than RSA in terms of storey shears and displacements at the upper storeys, as investigated by De Luca and Verderame (2013) [10]. The differences between LTHA and RSA can be still significant, especially at the lower storeys, when the input is given by a code-conforming approach represented by preassigned smoothed spectra, as investigated by De Luca and Lombardi (2017) [13]. The critical aspect for LTHA is the requirement for a proper input selection representative of the hazard at the site and subjected to the availability of ground motions. In the last decades, earthquake engineering has progressed significantly on the selection of ground motions mainly referring to Nonlinear Time-History Analyses (NTHA, e.g., McGuire 2004 [18]; Tothong et al. 2007 [19]; Iervolino et al. 2010a [20]; Baker 2011 [21]).

EC8 does not explicitly include LTHA among the seismic analysis methods in its latest version, released in 2004. ASCE/SEI 7-02 (ASCE 2003 [22]) already considered LTHA as an explicit option amongst the seismic methods of analysis but only recently a well-defined design procedure, proposed by Charney (2015) [12], is finally available for practitioners and engineers, and has been included in FEMA P-1050 (BSSC 2015 [23]) and ASCE/SEI 7-16. In these standards, the seismic input for LTHA design is given by a minimum of three spectrum-matched ground motions to replicate as closely as possible the typical outcome of RSA. This procedure, also known as spectral-matching, can be obtained by a wavelet adjustment procedure to closely match the smooth elastic acceleration response spectrum (i.e., code-based spectrum) for a range of periods. The benefit of using such a method is that the record-to-record variability is reduced considerably, and it is possible to obtain stable estimates (very similar to those obtained from RSA) of the mean response using a reasonably small number of structural analyses (Whittaker et al. 2011 [24]). However, this approach may not be consistent for specific conditions like near-fault earthquakes (e.g., Tothong et al. 2007 [19]; Chioccarelli and Iervolino 2010 [25]) as also specified in FEMA P-1050.

This paper aims to contribute to the development of design solutions towards a simplified EC8-compliant performance-based design framework using LTHA; first identifying the critical aspects preventing a widespread use of this analysis (i.e., ground motion selection for LTHA), and secondly providing a novel proposal to overcome those aspects that historically prevented practitioners from using such analysis for design. Section 2 presents a brief review of the current code-based practice for the selection of ground motions and the main differences between ASCE 7-16 (consistent with FEMA P-1050 document) and EC8. This section includes the description of different suites of ground motions for different field-conditions and selection criteria to investigate the optimisation of ground motion selection for LTHA design. In Section 3, a three-dimensional 12-storey archetype regular Reinforced Concrete (RC) Moment Resisting Frame (MRF) building designed according to EC8 through RSA is presented (De Luca and Lombardi 2017 [13]). This building is representative as a case study for which the higher-mode effects are shown to lead to significant differences between LTHA and RSA. This case study, together with others analysed in literature (i.e., steel MRF buildings in Aswegan and Charney 2014 [26]; BSSC 2016 [27]) are meant to enlarge the

practical examples of LTHA design. In Section 4, a novel framework for LTHA design, different from the prescriptions of FEMA P-1050 and fully compatible with EC8, is presented and it is applied to the case study. Aspects related to modelling and implementation of the proposed design framework are discussed. Design comparisons between LTHA and RSA (the latter assumed as conventional benchmark for the performance comparison) are shown and discussed in Section 5 for different suites made by seven pairs of ground motions, which is the EC8 minimum for averaging results of NTHA. Results are then extended with field-specific conditions (i.e., far-field, near-field and pulse-like conditions) in order to propose a general optimal input selection for LTHA design. Finally, conclusions and future developments are discussed in Section 6.

2. GROUND MOTION SELECTION FOR TIME-HISTORY ANALYSES

Many codes and standards allow practitioners to define the seismic input by using real, artificial or simulated (also known as synthetic) ground motions. Real ground motions are generally preferred by practitioners due to the difficulty of characterising seismological parameters when artificial and simulated motions are considered. Also, real ground motions are nowadays available from many databases, such as the PEER-NGA ground motion database (PEER NGA 2014 [28]), the European Strong Motion database (ESM 2008 [29]); they have the benefit of accounting for the real frequency content, the correct time correlation between the motion components and realistic energy content referred to seismological parameters. However, real ground motions are still limited in number and current procedures of seismic input selection for Time-History Analyses (THA) generally require manipulations of them.

In the following, a detailed discussion on the main code-based procedures for ground motion selection is presented. Particular attention is given to the procedures and provisions indicated in EC8 and FEMA P-1050, which are herein considered to select possible ground motion suites for LTHA design. It is highlighted that the current version of EC8, released in 2004, does not explicitly distinguish ground motion selection for LTHA and Nonlinear Time-History Analysis (NTHA). In fact, LTHA is not explicitly mentioned among the possible methods of seismic analysis. Therefore, the few available indications provided about the ground motion selection are generally referred to NTHA.

2.1 Selection approaches according to codes

The selection of ground motions depends on the goals of the analysis, which will generally be different for design and performance assessment (Whittaker et al. 2011 [24]). Indeed, if the goal of the analyst is, for example, the evaluation of the probability of collapse and related losses, then the record-to-record variability needs to be accounted for in the calculation of the structural response distribution (Cornell 2004 [30]). Generally, the input selection is referred to a specific target spectrum representative of the seismic hazard at the site (e.g., Iervolino et al. 2010a [20]). The target spectrum provided by many codes for design purposes, including EC8, is a Newmark-Hall functional spectral shape (e.g., McGuire 2004 [18]). Some standards, such as FEMA P-1050, allow also the use of the Uniform Hazard Spectrum (UHS) and the Maximum Considered Spectrum (MCE) as target spectra, the latter accounting for adjustment when sites are not near an active fault (Luco et al. 2007 [31]). The UHS has been used as a target spectrum in design practice for the past two decades (e.g., Calvi 2018 [32]) and it conservatively implies that large-amplitude spectral accelerations will occur at all periods within a single ground motion (Bommer et al. 2000 [33]). A better alternative, recently included in FEMA P-1050 and ASCE/SEI 7-16, is represented by the Conditional Mean Spectrum (CMS, Baker 2011 [21]; Jayaram et al. 2011 [34]; Goda and Atkinson 2011 [35]) which provides the expected response spectrum conditioned on the occurrence of a target spectral acceleration value at the period of interest.

In order to simplify the procedure of ground motion selection many tools have been developed and are freely available for practitioners (e.g., Iervolino et al. 2010b [36]; Cimellaro and Marasco 2015 [37]; Jayamon and Charney 2015 [38]; among others). Some procedures achieve the spectral-compatibility of real ground motions through linear scaling of the acceleration (i.e., so-called amplitude scaling). The ground motion is multiplied by a constant scaling factor so that the respective response spectrum and the target spectrum coincide at a specific period of vibration (generally the fundamental period of the structure, T_1), or such that the average of the scaled components from a suite of earthquakes closely matches (within some tolerance) the target spectrum in a specific range of periods of interest. It is preferable that the same scaling factor is applied to the two horizontal components and the vertical component to preserve the as-recorded

relationship between them. Experience has shown that not many ground motions are necessary to get the matching with the target spectrum, but a greater number of ground motions should be used if the intensity measure considered is not efficient and the effect on structural response of record-to-record variability needs to be captured (e.g., Tothong and Luco 2007 [39]; Kottke and Rathje 2008 [40]; Katsanos et al. 2010 [41]). The ideal scenario for a suitable ground motion selection approach for LTHA would be to be able to capture preliminarily information on the effect of record-to-record variability on the structural response but still to be compatible with the necessity to have a computationally efficient method for design (De Luca and Lombardi 2017 [13]).

As an alternative, some other procedures achieve the spectral-compatibility of real ground motions by wavelet adjustment (i.e., so-called spectral-matching) which, in principle, modifies the frequency content of a seed motion (Hancock 2006 [42]). Using spectral-matched ground motion as an input helps to reduce the variability in the seismic demand, and therefore allows fewer ground motions to be used to obtain stable estimates of the expected response (Hancock 2006 [42]). However, some studies have shown that wavelet-adjustment procedures can lead to some bias in terms of cyclic responses (e.g., Iervolino et al. 2010a [20]). It is worth noting that spectral-matching may not be appropriate for pulse-like motions (Whittaker et al. 2011 [24]). Spectral-matching is explicitly suggested as an approach for LTHA design in FEMA P-1050.

Table 1 compares the input selection approaches for EC8 and FEMA P-1050. EC8 provisions are implicitly referred to NTHA since LTHA is not mentioned explicitly among the possible methods of seismic analysis.

2.2 Ground motion suites for the case-study

Ground motion selection procedures require preliminary knowledge of the site and the modal properties of the structure of interest. The first step for the input selection is to determine the target spectrum for the considered limit state at the site. According to EC8, the elastic spectra should be obtained from the country's National Annex specifications (see Table 1). As shown in Section 3, the case study herein considered is represented by a multi-storey building located in Italy. The Italian National Annex specifications for EC8 design allow the definition of a site-dependent elastic response spectrum for the whole territory (Italian Building Code 2018 [6]; Meletti et al. 2007 [43]). This spectrum practically coincides with the UHS on rock for the site in question (Iervolino et al. 2010b [36]). Recently, a new seismic hazard model for Europe has been delivered (Woessner et al. 2015 [44]) which shows a generalised increase of PGA values with respect to the current Italian reference model. However, it has not yet been implemented in the most recent version of Italian code (Italian Building Code 2018 [6]).

The elastic spectrum can be built up for four limit states (two for serviceability and two for ultimate limit states) at sites in Italy, according to the information provided in the Italian code. For this study, the Life-Safety Limit State (10% probability of exceedance in 50 years) is considered. Furthermore, the ground motion selection requires a preliminary knowledge of the periods of vibration which affects the behaviour of the structure (i.e., definition of the lower and upper tolerances for spectrum-compatibility). The fundamental period of the structure can be roughly obtained from simplified equations, but only modal analysis can reveal which modes of vibration significantly contribute to the structural response. Therefore, in order to have results that are consistent with the structural members' capacities, pre-dimensioning of the structure is needed (for example, performed through LFM or even RSA).

Another important aspect herein pointed out is related to the shape of target spectra for sites nearby faults (e.g., Chioccarelli and Iervolino 2013 [25], Almufti et al. 2015 [45], Kohrangi et al. 2018 [46]). Most of the seismic design codes, including the Italian code, provide generic target spectra regardless of the closeness to the fault or directivity effects, etc. The selection of ground motions based on spectral shape is problematic for near-field regions and is still debated.

In order to evaluate the influence of the EC8-compliant ground motion selection on LTHA design, both in terms of demand and capacity, different suites of earthquakes are herein considered and described in the following. It is worth mentioning that, rigorously, ground motion selection should be building-, site- and intensity measure- specific. It should be carried out so that the seismogenetic features of the source and to the soil conditions of the site are accounted for, as also stated in EC8. However, the lack of sufficient recorded earthquakes for many sites makes it challenging, especially for medium-high seismic regions like the one herein considered. For this reason, the current practice is based on the selection of earthquakes from different sites as long as it satisfies the code-requirements, even if the selection does not meet the regional characteristics (Iervolino et al. 2010b [36]). This can be reasonable for design purposes and is generally accepted also for NTHA.

The selection accounts for different design conditions such as Unspecified-Field ground motions (in the following called UF), Far-Field ground motions (FF), Near-Field ground motions, both Pulse-Like and Not Pulse-Like (NFPL and NFNPL), and an *ad hoc* selection of ground motions with pulse period $T_P \leq T_1$ (PL). Some of the above suites are scaled (–S) and some others are unscaled (-U).

Table 1 Comparison between EC8 and FEMA P-1050 provisions on input selection.

Requirement	EC8	FEMA P-1050
Target Spectrum	Country's National Annex otherwise Type 1 (M>5.5) and Type 2 (M≤5.5) spectral shapes are defined. [§3.2.2.1(4)]	Method 1 (MCE) or Method 2 (CMS). However, UHS is allowed as well. [§16.2.2]
Structural model	2D and/or 3D and swap of the two horizontal motion components. [§3.2.3.1.1(2)P, §3.2.3.2]	3D and swap of the two horizontal motion components. [§12.9.2.2, §12.9.2.4, §16.3.1]
Matching procedure and number of ground motions	There is no explicit reference to the procedures allowed for ground motion manipulation. Minimum of 3 and: - if < 7 the envelope of the responses is used as design value; - if ≥ 7 the average of the responses is used as design value. [§3.2.3.1, §4.3.3.4.3(3)]	For LTHA: spectral-matching of 3 pairs only (from artificial or/and recorded) and the envelope of the responses is used as design value. [§12.9.2.3, §12.9.2.6] For NTHA: ≥ 11 ground motions, scaled or spectral-matched, and the average of the responses is used as design value. [§16.2.3.1, §16.4.1]
Matching tolerance	Average spectrum ≥ 90% of the target spectrum within [0.2T_1, 2T_1] with mean of the spectral acceleration at T = 0 ≥ a_gS for the site of interest, where a_gS is the peak ground acceleration. [§3.2.3.1]	For LTHA: average of the spectral-matched spectra ≥ 90% of the target spectrum within [0.8T_{lower}, 1.2T_1]. [§12.9.2.3.1] For NTHA: - average spectrum of the maximum-direction spectra ≥ 90% of the target spectrum within [T_{lower}, 2T_1]; [§16.2.4.1, §16.2.4.2]; - if spectral-matching is utilized, average spectrum of the spectral-matched components ≥ target spectrum within [T_{lower}, 2T_1]. [§16.2.4.1, §16.2.4.3]
Near-field conditions	No explicit mention of near-source conditions.	Spectral-matching shall not be utilized unless the pulse characteristics are retained after the matching. [§16.2.4.3] The rotation of the ground motion components to the fault-normal and fault-parallel directions is required, otherwise for all other sites they should be applied at arbitrary orientations. [§16.2.5.1]

*T_1 and T_{lower} are the fundamental and the lowest period required for the structural model to reach 90% total modal participation mass in each orthogonal direction (T_{lower} ≤ 20% of the minimum fundamental period between the two main directions), respectively.

2.2.1 Suite of Unspecified-Field Unscaled (UF-U) ground motions

A suite of seven pairs of unscaled real ground motions is selected from the European Strong Motion database (ESM 2008 [29]) to be spectrum-compatible with the target spectrum for the Life-Safety Limit-State (LS-LS). Such suites are meant to be selected without any distinction in terms of field conditions (i.e., "Unspecified-Field" condition). The selection of UF-U suite is performed through the Matlab-based software REXEL (Iervolino et al. 2010b [36]). REXEL allows to obtain the disaggregation of the seismic hazard at any site of interest in Italy. It results that for spectral acceleration corresponding to one second, the earthquakes contributing to the hazard at the site are in the intervals of moment magnitude and source-to-site distance equal to [4.5, 8] M and [0, 60] km, respectively. These intervals are assumed in the following for selecting possible ground motion suites. The spectrum-compatibility is performed so that the average of the selected ground motions (μ) matches the target spectrum between 10% lower and 30% upper tolerances over the period range [0, 4] seconds. It is worth noting that the 30% upper tolerance is not indicated by EC8, but it is suggested in Iervolino et al. (2010b) [36]. The goodness of the spectrum-compatibility can be observed in Figure 1a. Notwithstanding the good matching of the average spectrum to the target spectrum, the variability of the selected spectra is high, indicated in Figure 1a by the average ± one standard deviation ($\mu \pm \sigma$). However, standards and codes do not impose any restriction on the variability.

2.2.2 Suite of Spectral-Matched (SM) ground motions in accordance with FEMA P-1050 provisions

A sub-suite made of three pairs of ground motions from the UF-U described in Section 2.2.1 is selected to be compliant with the FEMA P-1050 provisions for LTHA. In the following it is called UF-SM (i.e., "Unspecified-Field-Spectral-Matched"). The spectral-matching is performed through the Spectrum Matching Toolkit (Jayamon and Charney 2015 [38]). The first ten modes of vibration are considered adequate for the benchmark building to cover higher-mode effects and to impose the period range for the matching. Figure 1b shows the goodness of the match according to FEMA P-1050. As expected, the variability is considerably reduced with respect to UF-U.

2.2.3 Suites of Unspecified-Field Scaled (UF-S) ground motions

In order to investigate the optimisation of the LTHA input selection and its effects on the results, two suites of seven pairs of scaled real ground motions are considered. The first suite is based on the UF-U suite described in Section 2.2.1, scaled in order to reduce the effect of the strongest ground motions and to still accomplish the spectrum-compatibility requirements (see Figure 1c), as explained in Section 5. This suite is referred to in the following as UF-S1. The second suite of scaled ground motion, selected from the latest version of the PEER NGA West2 ground motion database (PEER NGA 2014 [28]), presents a reduced record-to-record variability (see Figure 1d). It is called in the following UF-S2 and it is selected, based on the results of the disaggregation of the seismic hazard at the site of interest, to have compatible moment magnitude and source-to-site distance values. Further details about how the scaling is performed can be found in Section 5. It is worth noting that the 30% upper tolerance considered in Section 2.2.1 is not applied for these cases. Indeed, regarding this aspect, these selections are chosen with the intent of controlling the individual ground motions instead of their average.

2.2.4 Suite of Far-Field Uscaled (FF-U) and Near-Field Pulse-Like/Not Pulse-Like Unscaled (NFPL-U/NFNPL-U) ground motions from FEMA P-695

In order to increase the number of ground motions used to investigate the optimisation of the LTHA input selection and consider earthquakes that may be characterised by directivity effects (Somerville et al. 1997 [47]; Abrahamson 2000 [48]; Akkar et al. 2005 [49]; Luco and Cornell 2007 [50]), the far-field and near-field motion suites provided by FEMA P-695 (ATC 2009 [51]) are considered herein. The far-field suite includes 22 earthquakes from sites located at least 10 km from the fault rupture. The near-field suite includes 28 earthquakes from sites located within 10 km from the fault. From the latter suite, 14 earthquakes with strong pulses (called Pulse-Like) and 14 earthquakes without such pulses (called Not Pulse-Like) were judged by wavelet analysis classification (Baker 2007 [52]). Three suites are considered in this study: (i) the suite of

Far-Field Unscaled (called FF-U) ground motions; (ii) the suite of Near-Field Pulse-Like Unscaled (NFPL-U) ground motions; (iii) the suite of Near-Field Not Pulse-Like Unscaled (NFNPL-U) ground motions. These ground motions result compatible with the results of the disaggregation at the site in terms of moment magnitude and source-to-site distance values, and they are downloaded from the latest version of the PEER NGA-West2 ground motion database. Ground motions of the near-field conditions are rotated to the fault-normal (FN) and fault-parallel (FP) directions given the strike angle, according to FEMA P-1050. This is proposed because for sites located within 5 km of an active fault there is a tendency for response spectra to be larger in the FN direction than in the FP direction (Campbell and Bozorgnia 2007 [53]; Watson-Lamprey and Boore 2007 [54]). However, in some cases it is not true that the maximum amplitude of the acceleration is obtained along the FN direction. For these ground motions which exhibit directionality, the direction of maximum motion is generally aligned at varying azimuths. A more detailed discussion can be found in Stewart et al. (2011) [55]. EC8 does not provide any recommendations about this topic, so the approach suggested in FEMA P-1050 is adopted here. It is important to note that when performing analyses of buildings, swapping of the ground motions must be applied in order to adversely load both the main directions of the buildings.

Figure 1e-g show the goodness of the spectrum compatibility of the suites. The 30% upper tolerance of the average spectrum considered in Section 2.2.1 is not applied for these cases and the average spectrum of these suites is often significantly higher with respect to the target. These suites are considered in order to increase the number of ground motions for the calibration of an index that allows the input selection for LTHA design to be optimised, as explained in Section 5.

2.2.5 Suite of Pulse-Like Unscaled (PL-U) ground motions from Shahi and Baker's classification

Finally, a last suite of ground motions is considered herein to account for Pulse-Like motions which show relevant effects on the considered benchmark structure (called PL-U). Ten pairs of unscaled real ground motions are selected from the Shahi and Baker's classification (Shahi 2013 [56]) to be compatible with the results of the disaggregation at the site in terms of moment magnitude and source-to-site distance values, and they present a pulse period (T_P) smaller than the fundamental period of the structure (T_1), see Figure 1h. The ground motions present T_P between the period of the 3rd and the 6th mode of vibrations and elastic spectral accelerations between 0.4 g (RSN-415) and 3.5 g (RSN-4211) corresponding to T/T_P=1. In agreement with the previous section, ground motions are rotated to FN and FP directions. This suite is considered in order to increase the number of ground motions for the calibration of an index that allows the input selection to be optimised for LTHA design including pulse-like ground motions and making sure that the pulse characteristic has a significant effect on the response, as explained in Section 5.

3. EC8 DESIGN OF THE BENCHMARK BUILDING

In order to show the proposed EC8-compliant LTHA design procedure with a practical example, a case study structure in mid-high seismicity area is considered herein. The archetype structure is a regular 12-storey Reinforced Concrete (RC) Moment Resisting Frame (MRF) building (Figure 2), located in Pettino (L'Aquila, Italy) and designed through RSA with respect to the Ductility Class High (DCH) specifications according to EC8 (CEN 2004a [1]) and general rules related to RC structures according to EC2 (CEN 2004b [57]), including specifications of the Italian National Annex. Its design accounts for some aspects like the presence of a staircase, the maximum number of storeys resulting from ordinary concrete classes, relevant influence of higher-modes of vibration and significant P-Delta effects. Beam and column reinforcement and mechanical property details can be found in De Luca and Lombardi (2017) [13]. The behaviour factor q is equal to 5.85, it being a regular RC-MRF building. Design of irregular buildings is not herein investigated even though some indications are provided in the following.

Pulse-like earthquakes are considered herein to show limitations of the current codes. Indeed, EC8 does not provide any specific recommendations for near-fault regions. The benchmark building is located nearby an active fault (also known as Paganica fault, Akinci et al. 2009 [58]) and this can be particularly problematic for design.

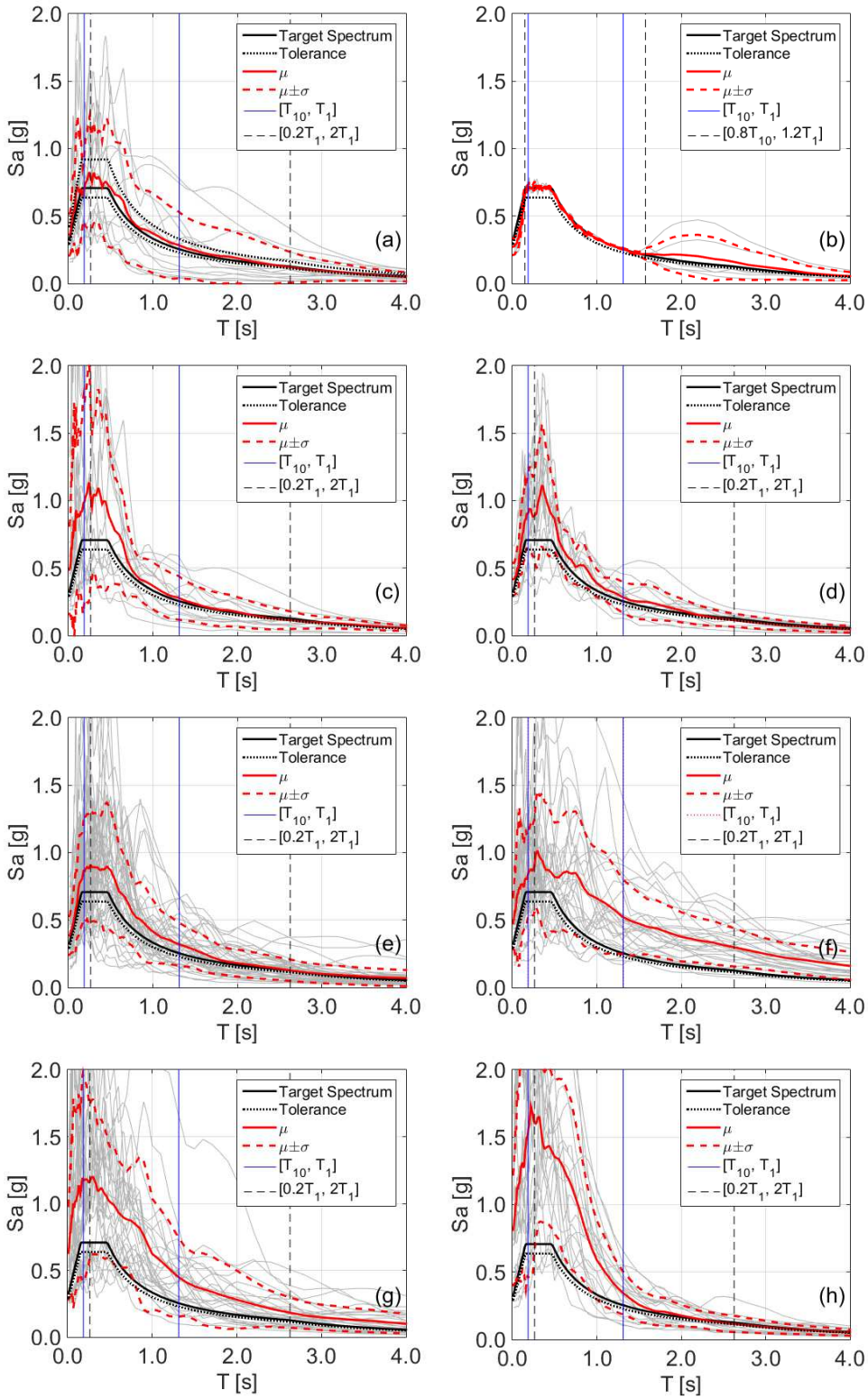

Figure 1 Ground motion selections for the suites of (a) UF-U, (b) UF-SM, (c) UF-S1, (d) UF-S2, (e) FF-U, (f) NFPL-U, (g) NFNPL-U, and (h) PL-U. [T_{10}, T_1] indicates the interval of the relevant periods of vibration of the benchmark building (see Section 3), where T_1 is the fundamental period and T_{10} the lowest period to satisfy the 90% total modal participation mass condition stated in Table 1.

4. THE PROPOSED EC8-COMPLIANT LTHA DESIGN PROCEDURE

Some current design codes (e.g., FEMA P-1050, BSSC 2015 [23]), excluding EC8, consider LTHA as an option among the seismic methods of analysis and some recommendations are provided for LTHA design. In this section, a new procedure for EC8-compliant "force-based" design is proposed and differences with respect to FEMA P-1050 are presented. The proposed procedure is presented for the LTHA design of the building described in Section 3, but it can be applied in general.

The structure represents an archetype, but it also includes some typical realistic design aspects that are encountered by practitioners (e.g., the presence of staircase). The proposed design procedure encompasses the relevant aspects discussed in EC8 and it provides recommendations on how to verify the structural compliance of structural members using the output of LTHA. Aspects such as: interaction between bending moments and axial force in the design of structural members, the estimation of P-Delta amplification factors, and the implementation of the behaviour factor are discussed and analysed in detail, providing a procedure for LTHA, analogous to the consolidated practice pursued in the case of RSA.

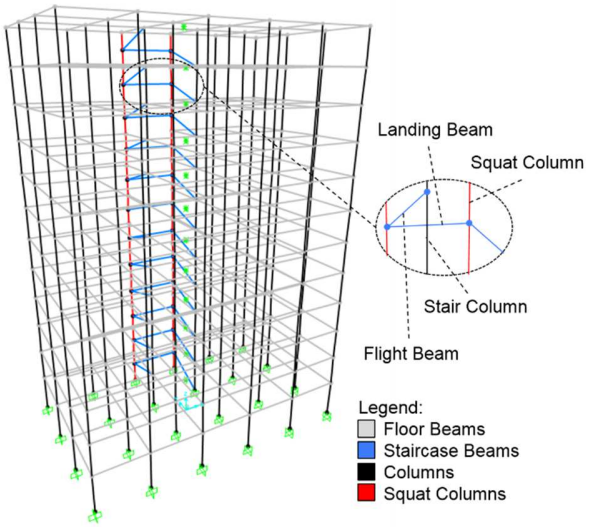

Figure 2 12-storey MRF case-study structure.

The proposed procedure is reported in Figure 3 and it can be split in three phases, namely Pre-Processing, Processing and Post-Processing for its implementation in software or routines. In the Pre-Processing, the numerical model, in terms of geometry, gravity loads, ground motion time-histories, and analysis features are defined. In the Processing phase, the gravity loads analysis and the time-history analyses are performed. In the Post-Processing phase, the results are analysed to evaluate P-delta effects, combinations of effects, and acceptance criteria. In order to make clear the explanation of the procedure, the Post-Processing is split in two parts (see Figure 3 and Figure 4).

4.1 Structural modelling

The benchmark building is modelled in OpenSees (OpenSees 2006 [59]) through "elasticBeamColumn" elements (see Figure 2). Concrete C35/45 is adopted for the whole building, resulting in a Young's Modulus E_c equal to 34.08 GPa calculated as per EC2. For concrete structures, cross-section flexural stiffness of members should account for an equivalent reduction of stiffness (e.g., from cracking). According to EC8, this can be obtained by reducing the flexural second moment of area and shear area each by 50%. Torsional stiffness should be accounted for by adopting a proper torsional constant value. Some commercial software uses the formulation reported in Young and Budynas (2002) [60] that is herein assumed.

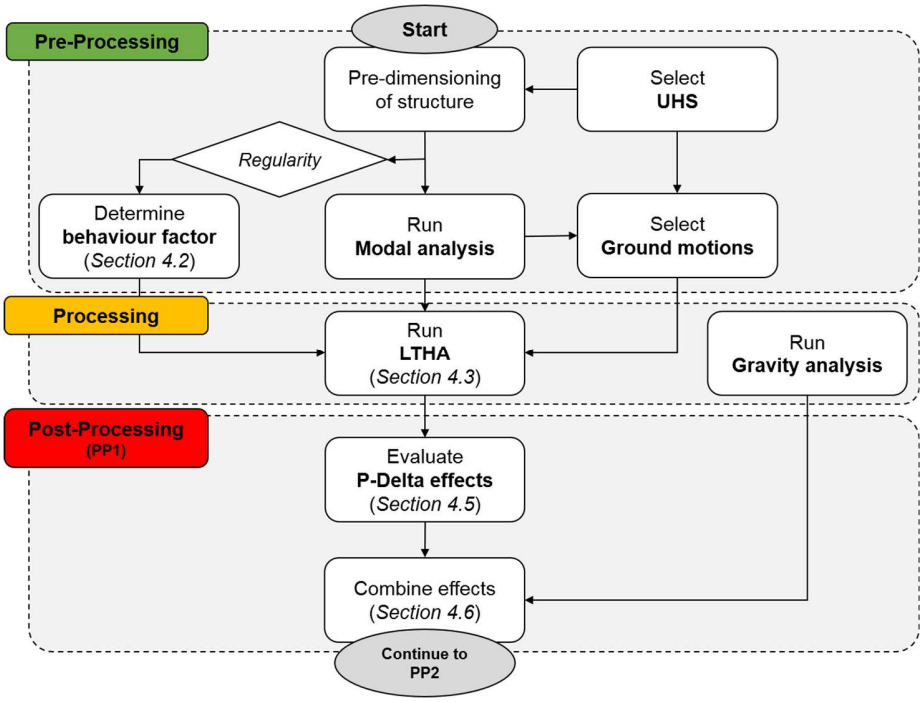

Figure 3 **Flowchart of the proposed LTHA design phases: pre-processing, processing and post-processing.**

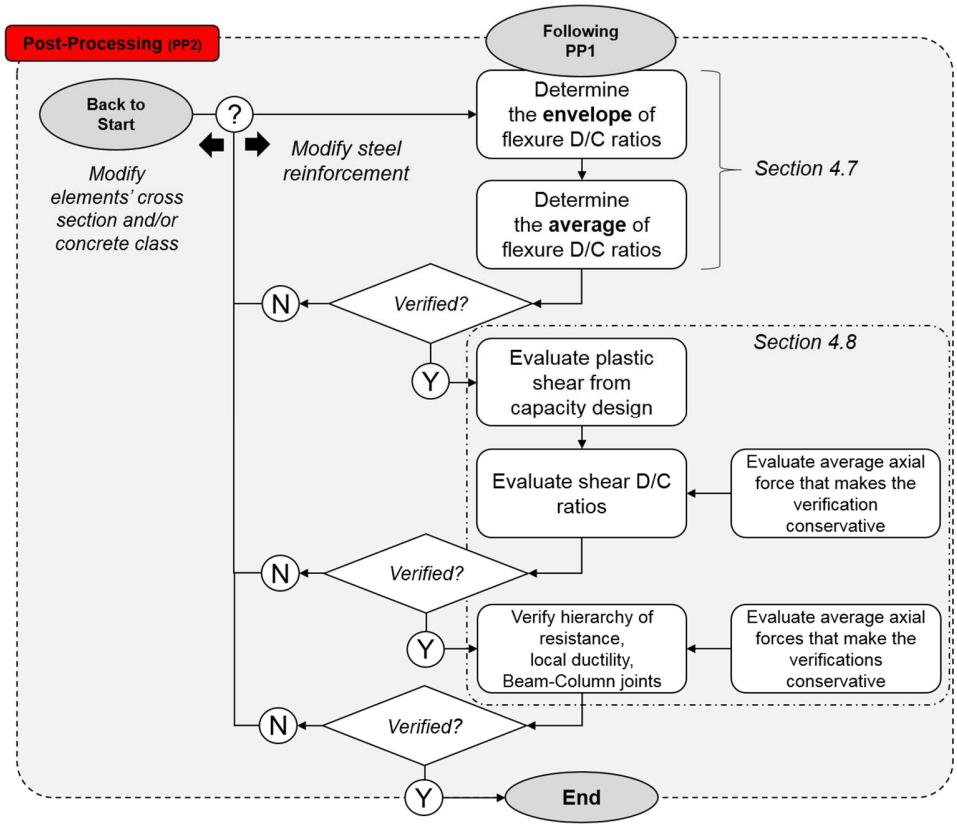

Figure 4 **Flowchart of the proposed LTHA design verification within the post-processing phase.**

Staircases or other members which affect the structural response should be accounted for in the model (Fardis 2009 [61]). The staircase considered in this study consists of inclined beams (flight beams) supporting the steps and supported, in turn, by members of the frame system. Such beams work in the strong direction of their cross-section as structural members subjected to the relevant interaction of axial force and bending moment. For simplicity the multi-linear beams (also known as "knee beams") are modelled as in the detail of Figure 2, through a whole inclined beam connecting the beam-to-column joints at the floor and landing levels (Fardis 2009 [61]). Storey diaphragms are assigned to each floor, except for the staircase landings for which the hypothesis is not applied. Floor loads, external infills and members' self-weight are assigned through distributed loads; members' self-weight mass is assigned as nodal mass to the ends of each member while floor and infill masses are lumped at the centre of mass of each storey, both evaluated according to the "half-and-half" seismic weight distribution criterion.

4.2 Behaviour factor

For typical force-based design approaches the elastic response spectrum for ultimate limit states is divided by the behaviour factor q in order to obtain the corresponding design demand on structural members. For the benchmark building q is equal to 5.85 (CEN 2004a [1]). However, for LTHA the spectrum-compatibility in ground motion selection is evaluated on the elastic response spectrum. For this reason, the time-histories can be divided by q. Herein, we propose a novel approach to conservatively evaluate the behaviour factor for LTHA (q_{LTHA}), defined as

$$q_{LTHA} = \min\left[S_{ae}(T_i)/S_{ad}(T_i)\right]_i \qquad \forall T_B \le T_i \le T_1 \tag{1}$$

where T_i is the period of vibration of the ith mode, $S_{ae}(T_i)$ is the value of the spectral acceleration corresponding to T_i evaluated on the elastic response spectrum (for the example presented here T_B is equal to 0.1568 s) and $S_{ad}(T_i)$ is the ordinate corresponding to the EC8 design spectrum (see Table 2 for their values) modified according to the Italian National Annex. Equation (1) identifies the minimum value of the behaviour factor all over the different spectral ordinates of the structure and then this value is applied to each one of the ground motion components, resulting in response spectra scaled by $1/q_{LTHA}$ (see Figure 5a-h). It is worth noting that the proposed approach keeps the validity of the spectrum-compatibility within the range of the relevant periods of vibration. Furthermore, this approach accounts for the imposed lower bound value of the pseudo-acceleration (i.e., $S_{ad}(T_i) \ge 0.2a_{g,\text{LS-LS}}$, where for the example presented here $a_{g,\text{LS-LS}}$ it is equal to 0.2604 g).

For the example presented here, q_{LTHA} is equal to 4.86 and it is applied to reduce the ground motion accelerations of any suite. This procedure allows the use of a behaviour factor that does not depend on the ground motion selection. The procedure according to FEMA P-1050 considers the modification of the response for inelastic behaviour *a posteriori*, by evaluating the maximum elastic base shear along each main direction (V_E) and multiplying it by I_e/R, where I_e is the importance factor and R the response modification factor (see FEMA P-1050 for how these parameters are evaluated). Then the base shear scale factor along each main direction (η) is evaluated as the minimum between 1.0 and the ratio between the base shears given by the static analysis and the one described above. This factor is utilised to determine the combined force response.

If the building is irregular in elevation, EC8 suggests reducing the value of the behaviour factor by 20% in order to get a higher seismic demand. Similarly, for buildings which are irregular in plan, the overstrength coefficient, denoted as α_u/α_1, is replaced by the average of its value and 1.0 as suggested in EC8. This approach can be applied also within the proposed procedure.

Finally, EC8 provides the upper limits of the behaviour factor that designers can use. In some cases, it may be useful to choose a more conservative value of the behaviour factor in order to increase the safety margins of the design (Fardis 2009 [61]). On the other hand, for conforming situations (i.e., reflecting the case of archetype regular structures), the values suggested by EC8 are generally lower than those evaluated through nonlinear analyses (e.g., Kappos 1999 [62], Elnashai and Mwafy 2002 [63]). The assumption in Equation (1) is consistent with the maximum value of q usable for RSA as the ground motion can be scaled by only one value while the response spectrum can be scaled by different q-values at different spectral ordinates. This is the case for the design of the benchmark building regardless of the assumption of q as the design spectrum cannot go lower than $0.2a_{g,\text{LS-LS}}$ and this limit affects the design. The behaviour

factor proposed for LTHA is valid regardless of the discretionary assumption made for q in RSA by the designer to determine the design spectrum.

4.3 Time-History Analyses

Thanks to the linearity of the analysis, each ground motion horizontal component can be applied independently along each of the main horizontal directions and subsequently combined with gravity loads analysis according to the superposition principle. Even if ground motions are applied independently along each direction, some torsional effects due to irregularity in plan are accounted for. For the example, the staircase clearly represents an irregular structural aspect within the behaviour of the building.
A direct-integration transient analysis method is used in OpenSees to solve the equations of motion of the structure subjected to dynamic loading. The Newmark method is used in OpenSees to numerically integrate the equations. The default parameters $\gamma = 0.50$ and $\beta = 0.25$ are assumed for the analyses.

Table 2 Periods of vibration (T_i), modal participation masses ($MP_{UX,i}$, $MP_{UY,i}$ and $MP_{RZ,i}$), and S_{ae} and S_{ad} corresponding to each period of vibration of the building.

Mode number, i	T_i [s]	$MP_{UX,i}$ [%]	$MP_{UY,i}$ [%]	$MP_{RZ,i}$ [%]	$S_{ae}(T_i)$ [g]	$S_{ad}(T_i)$ [g]
1	1.31	77.65	0.00	0.19	0.2532	0.0521
2	1.19	0.00	75.84	0.00	0.2796	0.0521
3	1.13	0.19	0.00	77.62	0.2945	0.0521
4	0.47	12.20	0.00	0.01	0.7074	0.1209
5	0.40	0.00	13.70	0.53	0.7074	0.1209
6	0.40	0.02	0.62	11.60	0.7074	0.1209
7	0.27	4.21	0.00	0.01	0.7074	0.1209
8	0.23	0.00	0.01	4.31	0.7074	0.1209
9	0.22	0.00	4.49	0.01	0.7074	0.1209
10	0.19	2.25	0.00	0.00	0.7074	0.1209
	∑	96.52	94.66	94.28		

4.4 Damping model

Many commercial software packages for structural analysis used by practitioners employ the Rayleigh damping model to evaluate damping forces in time-history analyses. This model is based on the user-definition of the damping ratios for only two periods of vibration while the damping ratios at other periods depend on the mass and stiffness proportional constants. The latter may lead to an underestimation of the response when higher modes are significant.
Also, the use of the Rayleigh damping model is not suggested for NTHA since it leads to “spurious” damping forces as shown in Chopra and McKenna (2016) [64]. For the benchmark building it results that the mass and stiffness proportional constants being equal to $\alpha_M = 0.2571$ rad/s and $\beta_K = 0.0097$ s/rad, respectively, when the damping ratios of the 1st and 3rd mode of vibration are each set to 5% (Chopra 2004 [4]). In this way, it would result in the damping ratio for the 10th mode being equal to 15%. The structural model herein analysed accounts for superposition of modal damping matrices (through the “modalDamping” command in OpenSees) and a damping ratio equal to 5% is adopted for each mode in accordance with the damping ratio used for the RSA, as also described in FEMA P-1050.

4.5 P-Delta effects

P-Delta effects are typically quantified through the evaluation of the interstorey drift sensitivity coefficient, denoted by ϑ. FEMA P-1050 provides a methodology in which P-Delta effects are directly included in the model by forming a constant geometric stiffness matrix created from gravity loads analysis (Wilson and Habibullah 1987; Wilson 2004). However, it was observed that because of the periods elongation of buildings it can lead to unconservative responses compared to the case without P-Delta effects (Aswegan

and Charney 2014 [26]). Otherwise, a static analysis is required by FEMA P-1050 to determine the interstorey drift sensitivity coefficient.

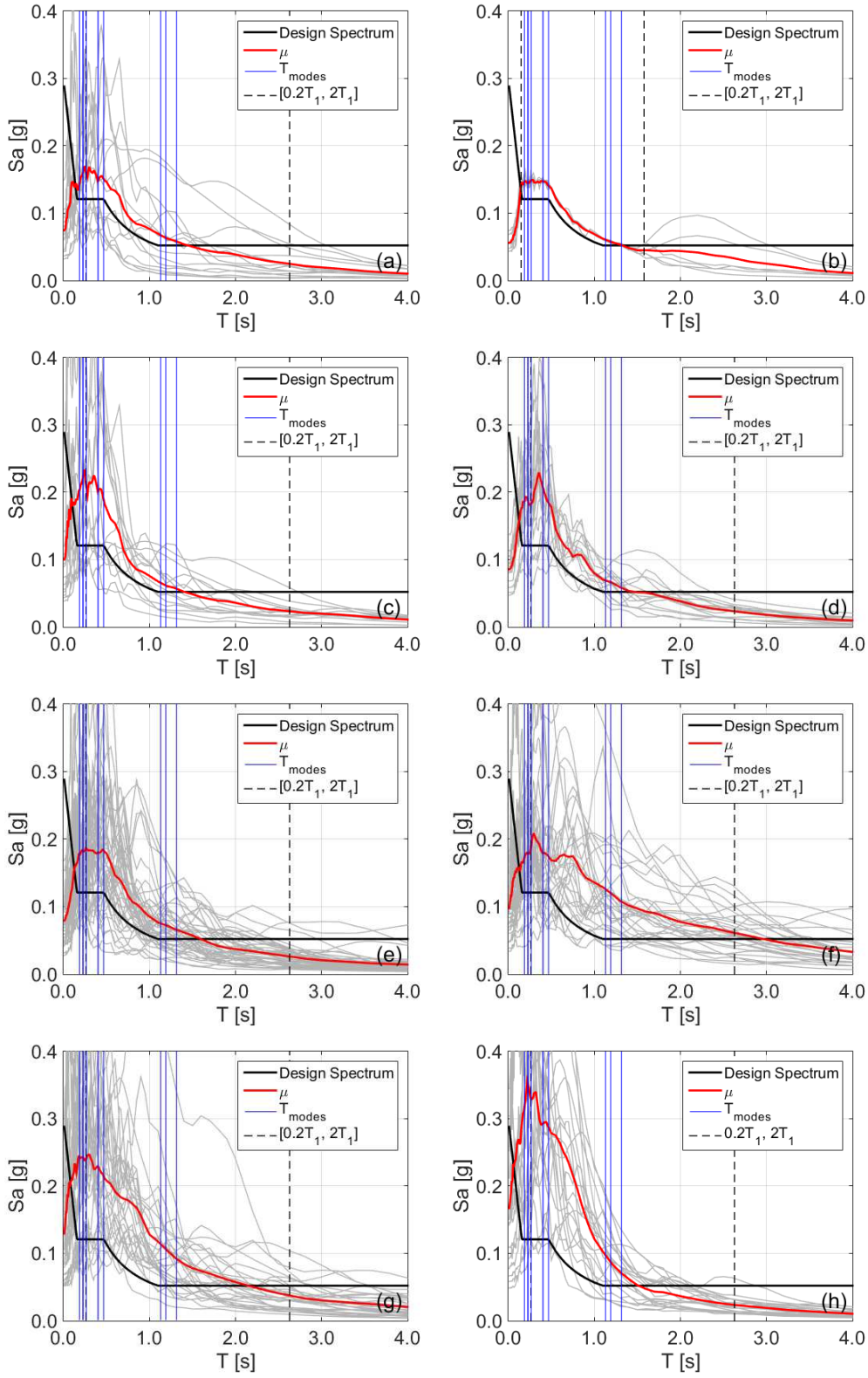

Figure 5 Comparison between code-design spectrum and ground motion design spectra for the suites of (a) UF-U, (b) UF-SM, (c) UF-S1, (d) UF-S2, (e) FF-U, (f) NFPL-U, (g) NFNPL-U, and (h) PL-U.

Herein, we propose to evaluate the P-Delta effects according to EC8 in the same way as considered for linear static analyses identifying the time step (t^*) for which the maximum interstorey drift ($d_{r,max}$) is achieved as:

$$\vartheta = P_{tot} d_r(t^*) \Big/ \left(V_{tot}(t^*) h\right) \qquad d_r(t^*) = d_{r,\max} \tag{2}$$

where P_{tot} is the total gravity load at and above the storey considered in the seismic design situations, h is the interstorey height, and $V_{tot}(t^*)$ is the storey shear corresponding to the maximum interstorey drift achieved over time (amplified by q for ultimate limit states according to the displacement rule when $T_1 \geq T_C$). The interstorey drift sensitivity coefficient can be evaluated for each horizontal ground motion component, in the two main directions. The amplification factor value, defined as $1/(1-\vartheta)$, equal to the maximum one evaluated between the two main directions among the storeys can be considered for each earthquake so that the equilibrium and coupling of ground motion components is preserved (Fardis 2009 [61]). The amplification factor can be applied *a posteriori* when performing the combinations of the unidirectional responses for each earthquake within the ground motion suite. In this way, the amplification of the effects is applied excluding the contribution of the gravity loads. For the earthquakes considered in the current example, the amplification factor varies between 1.00 and 1.12.

4.6 Seismic load combinations

Once the unidirectional responses have been obtained and the amplification factor to account for the P-Delta effects has been evaluated from them, the seismic combinations (Giannopoulos et al. 2018 [65]), with gravity loads included, can be performed to evaluate the most unfavourable effects (e.g., maximum/minimum local forces, displacements, reactions, etc.). For each earthquake (i.e., pair of horizontal ground motions), this procedure results in eight possible combinations of the horizontal ground motion components with swap of the single components ($\pm C1_{XorY}$ $\pm C2_{YorX}$), if accidental eccentricity is neglected. If accidental eccentricity is accounted for through a shift of the centre of mass, as also described in FEMA P-1050, it results in 8 x 5 = 40 (4 cases with the centre of mass shifted by 5% and one without shift) possible combinations. It is worth noting that the shift of the centre of mass changes the modal characteristics of the structure (De La Llera and Chopra 1994 [66]), and it inevitably leads to greater number of analyses to perform. Several procedures have been recently proposed to account for the effects of torsional ground motion in time-history analyses (e.g., Basu et al. 2014 [67]) but the current design codes do not include any of them. One aspect to note is that the ground motion components are combined by applying simultaneously 100% of their effects along the two orthogonal directions as per NTHA; so that occurrence of more than one component can be handled rigorously avoiding the application of the 100:30 combination rule employed for RSA (Fardis 2009 [61]).

4.7 Acceptance criteria

One of the benefits of performing LTHA is the possibility of calculating Demand/Capacity (D/C) ratios of effects (e.g., bending moments, interstorey drifts, etc.) step by step in the time domain for each seismic combination, by accounting for the actual interaction between bending moments and axial forces, if, obviously, the coupling between the as-recorded ground motion components is preserved (as considered in the proposed procedure). Even though this operation can be time consuming, this is an important aspect when capacities depend on demand such as the case of bending moment capacity depending on axial load. Design of members typically starts by considering their flexural behaviour. The proposed procedure is summarised in Figure 4 and it is based on the following steps:

- the maximum flexural D/C value of each member, among the seismic combinations, should be evaluated for each earthquake so that the envelope accounts for the actual interaction between bending moments and axial force. For columns, the flexural D/C ratio is evaluated separately in each direction with the uniaxial moment of resistance reduced by 30% (as suggested by EC8) to account

for the biaxial bending. Strictly speaking, the flexural *D/C* ratios should be evaluated step-by-step for each combination of the components of ground motions, then assuming the envelope for each earthquake for the average evaluation. It is suggested herein that the maximum value of flexural *D/C* over the earthquake duration should be considered. Also, because the single earthquakes are not spectrum-compatible when independently analysed, it might result that members fail under compression or tension. In these cases, the acceptance criteria can be changed in terms of axial *D/C*. For pure compression the *D/C* ratio can be evaluated as $N_{Ed}(t)$ / $0.55N_{Rd,c}$ (for DCH it is assumed normalised axial force limit ν = 0.55), where $N_{Rd,c}$ is the compressive axial capacity given by the concrete contribution only. For pure tension the *D/C* ratio can be evaluated as $N_{Ed}(t)$ / $N_{Rd,t}$, where $N_{Rd,t}$ is the tensile axial capacity given by the yielding of the reinforcement only;

- the average flexural *D/C* value of each structural member, within the ground motion suite, should be obtained and judged by the designer. It is suggested to avoid calculating "decoupled" flexural *D/C* ratios by calculating the average values of max/min axial loads and bending moments (which very likely are not coupled) since this operation generally leads to overconservative designs.

For the example presented here, the flexural capacity of members is evaluated through fibre-based section analysis. The concrete cross-section is discretised in a sufficient number of longitudinal fibres, having the Mander monotonic stress-strain relation (Mander et al. 1988 [68]). Confined concrete behaviour is assigned to the fibres within the area defined by the transversal steel reinforcement. Fibres, having the Menegotto-Pinto monotonic stress-strain relation (Menegotto and Pinto 1972 [69]), account for the longitudinal steel reinforcement, including side bars. Concrete and steel strengths refer to the corresponding design values. For unconfined concrete, the design strength is evaluated as $0.85f_{ck}$ / γ_C, where f_{ck} is the characteristic compressive cylinder strength (equal to 35 MPa) and γ_C is the partial factor for concrete (equal to 1.50). For confined concrete, the design strength is evaluated according to EC8-3 specifications (CEN 2005). For steel reinforcement, the design strength is evaluated as f_{syk} / γ_S, where f_{syk} is the characteristic yield strength (equal to 450 MPa) and γ_S is the partial factor for reinforcing steel (equal to 1.15). The axial force acting on the cross-section is accounted for in the flexural capacity evaluation. The verification is expressed in terms of *D/C* ratio evaluated for each member at its ends and for each seismic combination and time-step.

4.8 Capacity design, hierarchy of resistance and other verifications

Once the flexural design is performed and cross-sections of structural members are defined in terms of longitudinal reinforcement, the design shear forces (also known as plastic shears) can be determined in accordance with the capacity design rule. The capacity models for shear currently available in the literature do not account for biaxial loading conditions. For this reason, the shear *D/C* ratios are separately referred to each local axis of the cross-section. For simplicity, the design shear forces of members subjected to axial force can be calculated from the average value of the axial force acting at each end of the member that maximises the shear demand. The shear capacity can be simply calculated from the average value of the axial force acting at each end of the member that minimises the shear capacity. The shear capacity can be calculated according to the truss model with variable inclination (CEN 2004b [57]). The strut angle is assumed equal to 45 degrees for beams while it can change for columns, according to EC8 prescriptions for DCH. Capacity design can be checked considering the average axial force that minimises the values of the resisting bending moments in columns at the considered end. For beam-to-column joint verifications, the joint capacity can be calculated from the average axial force that makes the verification conservative.

4.9 Unacceptable cases

Because of the use of a linear-elastic model, it may result that the average *D/C* ratios for the selected suite of ground motions are very large. This aspect mainly depends on the earthquake spectra that show significant differences with respect to the design response spectrum. Specifically, the average *D/C* ratios can be significantly dependent on the largest *D/C* ratios (outliers) related to the ground motions, applied along a certain direction, that significantly amplify the structural response, leading to over-dimensioning of members and, hence, expensive design solutions. These cases are herein referred as "unacceptable cases" in the LTHA context when using "force-based" design and they are related to situations in which a building designed as EC8-compliant through RSA (as in this case) shows disproportionate and unrealistic

high values of DCR. The use of the lexical expression “unacceptable cases” recalls the meaning of this expression in the context of NTHA and its discussion in the ASCE/SEI 7-16 and FEMA P-1050.

Similarly to the index proposed by Jayaram et al. (2011) [34] to quantify the similarity between a ground motion response spectrum and the target one for NTHA ground motion selection, a new index is herein proposed to control the effects on the structure of each earthquake ground motion in the selected suite. This approach is based on the evaluation of the weighted average of the differences (or errors) of the spectral accelerations corresponding to each relevant period of vibration of the structure through the ground motion index:

$$I_{eq,j} = \sum_{i=1}^{n_p} \left[P_i \left(S_{ae,eq,j}(T_i) - S_{\text{a,target}}(T_i) \right) \right] \Big/ \sum_{i=1}^{n_p} P_i \qquad P_i = \sqrt{MP_{UX,i}^2 + MP_{UY,i}^2 + MP_{RZ,i}^2} \qquad j = 1,2 \qquad (3)$$

where P_i is the weight of the ith period of vibration (T_i), which is defined in terms of the modal participation masses of the mode, $S_{ae,eq,j}$ (T_i) and $S_{a,target}$ (T_i) are the ground motion and target (design for ultimate limit states) spectral accelerations corresponding to the ith mode, and n_p the number of relevant modes of vibration. Using the rigid diaphragm assumption, the weight of each mode can be expressed as the root mean square of the two translational ($MP_{UX,i}$ and $MP_{UY,i}$) and one rotational ($MP_{RZ,i}$) modal participation masses related to the in-plane displacements *UX* and *UY* and rotation *RZ*, respectively. Figure 6 shows an example of evaluation for I_{eq} according to Equation (3) for the benchmark building and three ground motions depicted in Figure 6a. Modal analysis properties of the first ten modes are those reported in Table 2 while other parameters are reported in Table 3. Figure 6b shows the differences in terms of spectral acceleration between ground motion spectra and target spectrum for simplicity denoted as $Diff(T_i)$ while Figure 6c shows such differences multiplied by the modal weight P_i. Results show that earthquake #1 (grey line and dots), which response spectrum is significantly below the target one, presents spectral differences at the relevant periods always negative, and I_{eq} equal to -0.0402 g; it is expected that it would lead to low values of *D/C* ratios for a building initially designed through RSA and that target spectrum. Differently, earthquake #3 (blue line and dots), which response spectrum is closer to the target one, presents positive spectral differences and I_{eq} equal to +0.0339 g; it is expected that this earthquake would lead to *D/C* ratios larger than earthquake #1 but comparable to RSA design. Finally, earthquake #2 (red line and dots) presents response spectrum higher than the target one and larger positive spectral differences at the first three periods than earthquake #3; this earthquake shows the largest I_{eq}, being equal to +0.0976 g and it is expected that it would lead to the largest D/C ratios compared the previous earthquakes and RSA design. For the sake of ground motion selection optimisation, earthquake #2 could be erased from the suite (or scaled by <1) and replaced with another one showing lower index value.

Figure 6b-c show the small “correction” of the differences in terms of spectral acceleration at the periods which show larger modal participation masses (i.e., predominant modes), and the large “correction” of such differences at the periods which show smaller modal participation masses (i.e., higher modes) but still relevant. For earthquake #3 such “correction” shows that higher modes contribution is still relevant compared to the other ones, as confirmed by the blue dots at the 4th to 6th periods of vibration.

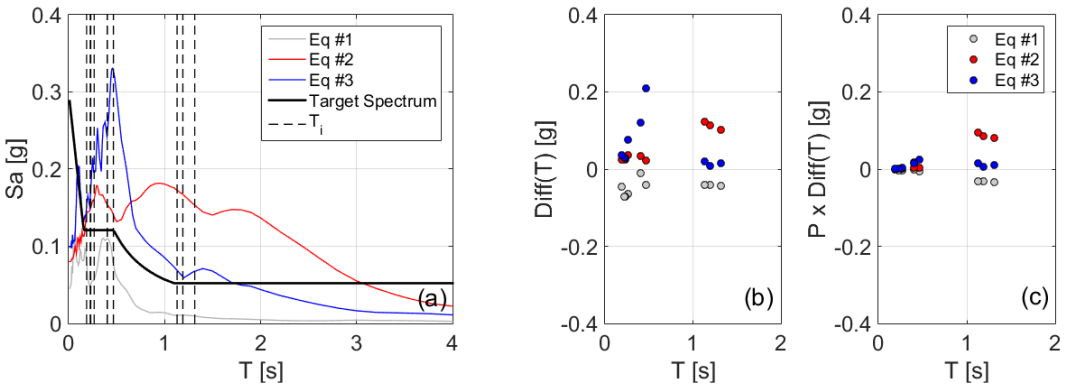

Figure 6 Example of evaluation for I_{eq}: (a) ground motion spectra of three earthquakes compared to the target spectrum, (b) differences at the relevant periods in terms of spectral

accelerations for simplicity denoted as $Diff(T_i)$, and (c) same differences multiplied by the modal weight P_i of the building.

This example shows that if the designer aims at selecting an optimal ground motion suite, the ground motions having large positive I_{eq} value could be scaled down (i.e., scaled by <1) while ground motions having large negative I_{eq} value could be scaled up (i.e., scaled by >1).

4.9.1 Limits of I_{eq}

Equation (3) assumes that the same ground motion component is applied along both the main directions of the building since the spectral acceleration differences at the relevant periods are evaluated from the same ground motion spectrum. However, swapping of the ground motion components is always required when analyses are performed, therefore, this can be assumed if the maximum I_{eq} between the two components (i.e., j = 1,2) is considered for a generic earthquake.
Contrarily to Jayaram et al. (2011) [34], the index in Equation (3) avoids using the sum of the squared differences in order to keep the sign (+/-) of the differences at multiple spectral ordinates and it is inspired by the approach used in Shome and Cornell (1999) [70] in which the weighted average of the spectral accelerations at the first three modes was used as intensity measure to get a substantial reduction in dispersion with respect to the normalisation at the first-mode spectral acceleration.
The following aspects should be considered when using Equation (3):

- for some conditions the evaluation of I_{eq} can lead to cancelation of the differences at different periods for "as-recorded" ground motions. The condition $I_{eq} \approx 0$ is not therefore equivalent to the "ideal" condition of matching the target spectrum through a spectral-matching procedure;
- I_{eq} is proposed for three-dimensional buildings where more than two periods of vibration and swapping of the horizontal ground motion components are both considered;
- there is not a unique relationship between I_{eq} and the effects of ground motions (i.e., two earthquakes can certainly show similar values of I_{eq} but different effects on the same structure).

Table 3 I_{eq} for the benchmark building and three ground motions depicted in Figure 6: P_i is the modal weight expressed in terms of modal participation masses (see Table 2), and $S_{ad,target}(T_i)$ and $S_{ad,eqj}(T_i)$ are the design spectral accelerations corresponding to each period of vibration of the building (T_i) evaluated on the target spectrum and the ground motion spectrum j, respectively.

Mode number, i	P_i	$S_{ad,target}(T_i)$ [g]	$S_{ad,eq1}(T_i)$ [g]	$S_{ad,eq2}(T_i)$ [g]	$S_{ae,eq3}(T_i)$ [g]
1	77.65	0.0521	0.0099	0.1546	0.0670
2	75.84	0.0521	0.0108	0.1661	0.0591
3	77.62	0.0521	0.0104	0.1754	0.0730
4	12.20	0.1209	0.0808	0.1427	0.3311
5	13.71	0.1209	0.1100	0.1540	0.2421
6	11.62	0.1209	0.1100	0.1540	0.2421
7	4.21	0.1209	0.0556	0.1582	0.1963
8	4.31	0.1209	0.0485	0.1458	0.1511
9	4.49	0.1209	0.0485	0.1458	0.1511
10	2.25	0.1209	0.0747	0.1453	0.1574

4.9.2 I_{eq} versus $I_{eq,SRSS}$

In the following, the proposed I_{eq} is compared to $I_{eq,SRSS}$, the latter implementing the Square Root of the Sum of Squares (SRSS) of the spectral differences (i.e., $Diff(T_i)$ for i = 1,…,n_p) as per Equation (4). The SRSS of the spectral differences is a well-established approach for ground motion selection strategies in literature (e.g., Naeim et al. 2004; Jayaram et al. 2011). For this reason, this section is meant to investigate the suitability of I_{eq} and $I_{eq,SRSS}$ for the purpose of LTHA ground motion selection.

$$I_{eq,SRSS,j} = \sqrt{\sum_{i=1}^{n_p}\left[P_i\left(S_{ae,eq,j}(T_i) - S_{\text{a,target,j}}(T_i)\right)^2\right] \Big/ \sum_{i=1}^{n_p} P_i} \quad (4)$$

I_{eq} and $I_{eq,SRSS}$ are evaluated for each ground motion component of the suites described in Section 2.2. The comparison is showed in Figure 7a in terms of I_{eq} versus $I_{eq,SRSS}$ for the same ground motion component. It is possible to observe that $I_{eq,SRSS}$ always provides larger values than I_{eq} as confirmed by the points located above the bisectors. For ground motion spectra characterised by always positive spectral differences (i.e., $S_{ae,eq}(T_i) > S_{a,target}(T_i)$) the two indexes tends to align along the right-hand bisector. In analogy, for ground motion spectra characterised by always negative spectral differences (i.e., $S_{ae,eq}(T_i) < S_{a,target}(T_i)$) the two indexes tends to align along the left-hand bisector. However, when the spectral differences are negative and positive at different periods, $I_{eq,SRSS}$ tends to divert from I_{eq}. In order to quantify the differences between I_{eq} and $I_{eq,SRSS}$, the Pearson's linear correlation coefficient, denoted by ρ is evaluated for each ground motion suite (see Figure 7b). From Figure7b, it is possible to observe that the correlation between I_{eq} and $I_{eq,SRSS}$ is always positive for the selected suites in this paper and it is small for the optimised ground motion suite UF-S2 being $\rho = 0.14$. On the contrast, when ground motions are selected to be higher with respect to the target spectrum, e.g. NFPL-U, the correlation between I_{eq} and $I_{eq,SRSS}$ is large being $\rho = 0.85$.

The $I_{eq,SRSS}$ implements the SRSS of the spectral differences that has been widely applied for NTHA ground motion selection. It is difficult to state if I_{eq} can provide a better performance in ground motion selection than $I_{eq,SRSS}$. However, I_{eq} having the sign is more informative than $I_{eq,SRSS}$ for potential scaling or changes of single ground motions within a suite.

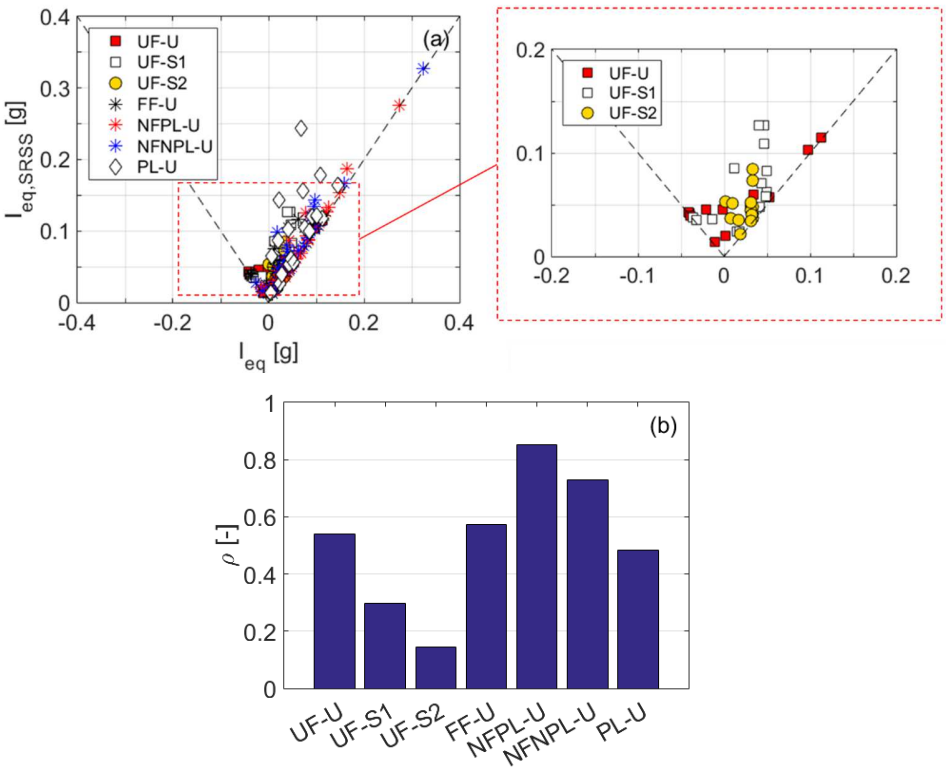

Figure 7 I_{eq} **versus** $I_{eq,SRSS}$**: (a) values of the indexes for each ground motion component of the suites, and (b) Pearson's linear correlation coefficient (**ρ**) for each ground motion suite.**

5. PERFORMANCE COMPARISONS

In this section, results obtained from LTHA design for the different suites are compared to those obtained from RSA for the analysed benchmark building and discussed in Section 5.1. Results are then extended considering suites of unscaled real ground motions for specific-field conditions (far-field, near-field pulse/not pulse-like and pulse-like with $T_P \leq T_1$) and they are fitted through linear regression in the semi-logarithm space of the maximum Demand/Capacity (D/C) ratio versus the maximum ground motion index I_{eq} for each earthquake (i.e., $\log(D/C)_{max}$ vs $I_{eq,max}$), as described in Section 5.2.

5.1 Design comparisons (RSA vs LTHA)

Figure 8 shows the maximum flexural D/C ratios evaluated at each storey for different groups of structural members, as indicated in Figure 2 (i.e., floor beams, staircase beams, columns, and squat columns), in the cases of ground motion suites assumed for design (i.e., RSA, UF-U, UF-S1, UF-S2, and UF-SM).
The results are obtained by checking the RSA design through LTHA for the sake of comparison. These results show that the benchmark building designed through RSA, presents insufficient longitudinal reinforcement in most beams and columns when it is checked through LTHA, according to both the spectral-matching procedure proposed by FEMA P-1050 (namely UF-SM) and the spectrum-compatibility procedure proposed for NTHA by EC8 (namely UF-U, UF-S1, and UF-S2). Failures seem to be particularly critical for beams and columns of the staircase (e.g., flight beams and squat columns in Figure 8). These members are subjected to high axial forces (both of tension and compression) and bending moments. In fact, the average values of the D/C ratios in terms of flexure for these members are highly dependent on the strongest earthquakes within the ground motion suites (i.e., the outliers of the suite of ground motions). Generally, real ground motions present spectral shapes that are very likely to be dissimilar to the target spectrum given by design codes. In order to accomplish the spectrum-compatibility requirements, spectral shapes can be much higher than the target spectrum in specific ranges of period of vibration, resulting in being very high in demand for members if significant modes of the structure fall within these ranges. The spectral-matching procedure (here adopted for the suite UF-SM) is convenient for designers but it presents limits when specific-field conditions in relation to faults have to be accounted for (BSSC 2015 [23]).
In the following, it is shown that it is possible to control LTHA results and obtain convenient design solutions when the suggested ground motion index (I_{eq}) in Equation (3) is considered for the input selection. The index I_{eq} is found to be a good indicator of the effect of a certain ground motion on LTHA design. Table 4 reports I_{eq} evaluated for each earthquake ground motion component of the considered suites. Comments for each design solution are presented in the following:

- UF-U (Figure 1a and Figure 5a): it was found that the average D/C ratios in terms of flexure are strongly influenced by earthquakes 4 and 7, which have the largest values of $I_{eq,max}$ (i.e., the maximum value of I_{eq} between the two ground motion components for each earthquake), equal to +0.0976 g and +0.1124 g respectively (see Table 4). Re-design of the members showing D/C ratios greater than unity leads to increasing longitudinal steel reinforcement in beams and, in turn, increasing longitudinal and transversal steel reinforcement in columns, especially those of the staircase. However, it results problematic with this assumption satisfying the verification of beam-to-column joints. This issue would scrupulously suggest changing structural system of the staircase to reinforced-concrete shear walls as typically adopted in practice for medium-high rise buildings.
- UF-S1 (Figure 1b and Figure 5b): in order to investigate other structural solutions which can lead to a cheaper design than UF-U, UF-S1 suite was obtained scaling linearly the UF-U suite still keeping it spectrum-compatible. The aim was reducing the effects of the strong earthquakes (i.e., 4 and 7 in suite UF-U) by scaling them without amplifying significantly the other ones within the same suite. The scaling factors used for each couple of ground motions ranged between 0.60 and 4.50. These values are consistent with the results found in Luco and Bazzurro (2007) [71] related to the maximum usable scaling factors to avoid biased results. After the scaling, the average D/C ratios in terms of flexure are mostly dependent on earthquakes 1, 3, and 4 which show the largest D/C ratios and have $I_{eq,max}$ equal to +0.0491 g, +0.0492 g, and +0.0489 g respectively (see Table 4). Even after this scaling of the ground motions, the design of beams and columns of the staircase is still very critical (see Figure 8).
- UF-S2 (Figure 1c and Figure 5c): this suite leads to more convenient results than UF-U and UF-S1 as also shown by the largest $I_{eq,max}$ that is equal to +0.034 g being smaller with respect to the

previous cases (see Table 4). The scaling factors for UF-S2 ranged between 1.18 and 2.50. This suite also presents lower record-to-record variability than UF-U and UF-S1 as shown by the $\mu \pm \sigma$ trend in Figure1d and Figure 5d. Even if results of the UF-S2 suite are still not acceptable for design (because *D/C* ratio values are greater than one), they are less critical than the previous cases (i.e., the largest D/C ratio value is about 1.70 and it refers to the flight beam at the 2nd storey) and certainly more convenient from the economic point of view, resulting in acceptable modifications to the reinforcement of members compared to RSA design, as shown by Figure 8.

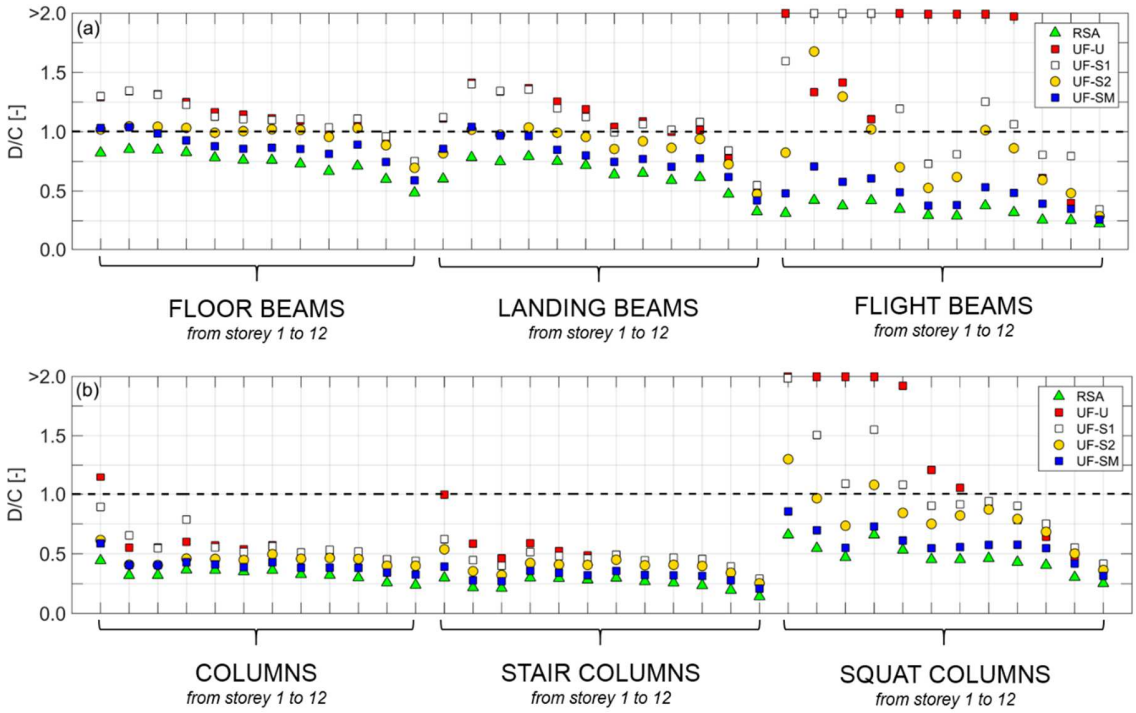

Figure 8 Design *D/C* ratios in terms of flexure for (a) beams and (b) columns (for RSA and UF-SM the results refer to the envelopes, for UF-U, UF-S1 and UF-S2 to the averages).

5.2 Fitting of results and I_{eq} optimum value

A linear regression of the results in the semi-logarithm space of the maximum flexural *D/C* ratio versus the maximum ground motion index I_{eq} for each earthquake (i.e., $\log(D/C)_{max}$ vs $I_{eq,max}$) and its confidence bands are obtained in order to calibrate an optimum value of I_{eq} that can be used as a target value for designers considering ground motion selection for LTHA (see Figure 9).

Table 4 Ground motion index I_{eq} evaluated for the different suites of ground motions.

Suite	*Ground Motion Component*	*Earthquake Number (EQ)*						
		1	2	3	4	5	6	7
UF-U	1	0.0491	-0.0402	0.0302	0.0976	-0.0390	-0.0210	-0.0107
	2	-0.0142	-0.0415	0.0017	0.0527	0.0339	-0.0011	0.1124
UF-S1	1	0.0491	0.0461	0.0492	0.0489	-0.0364	0.0119	-0.0324
	2	-0.0142	0.0402	0.0151	0.0174	0.0437	0.0468	0.0415
UF-S2	1	0.0333	0.0333	0.0334	0.0078	0.0307	0.0171	0.0315
	2	0.0331	0.0313	0.0015	0.0326	0.0192	0.0328	0.0099

This operation is performed for the different groups of structural members identified within the building (see Figure 2): floor beams, staircase beams, squat columns, and other columns. Different suites of unscaled ground motions belonging to specific-field conditions were considered (i.e., FF-U, NFPL-U, NFNPL-U and PL-U). A total of 84 earthquakes were considered for the fitting (i.e., 7 from UF-U, 3 from UF-SM, 7 from UF-S1, 7 from UF-S2, 22 from FF-U, 14 from NFPL-U, 14 from NFNPL-U, 10 from PL-U) plus the results obtained from RSA. This allows designers to infer the expected range of the maximum flexural *D/C* ratio value for a certain ground motion within a selected suite, represented by the index in Equation (3). The best fit relationship between the $(D/C)_{max}$ and $I_{eq,\max}$ is presented in the form of Equation (5):

$$\log\left(D/C\right)_{\max} = a\, I_{eq,\max} + b \tag{5}$$

where *a* and *b* are the values reported in Figure 9 for each member group. Linear regressions of the results show values of R^2 equal to 0.82, 0.47, 0.52 and 0.76 for floor beams, staircase beams, squat columns and other columns, respectively. While for floor beams and other columns the goodness of the linear regressions can be considered accurate (i.e., R^2 values closer to unity), for staircase beams and squat columns the distribution of the *D/C* values is particularly affected by their higher values (as confirmed by the low values of R^2, i.e. 0.47 and 0.52). Results show that a value of $I_{eq,\max}$ equal to 0.03 g can be suggested as target value for ground motion selection leading to alternative design options that can be still considered economically-feasible in professional applications (i.e., convenient changes in the dimensions or reinforcements of the members with respect to the RSA).

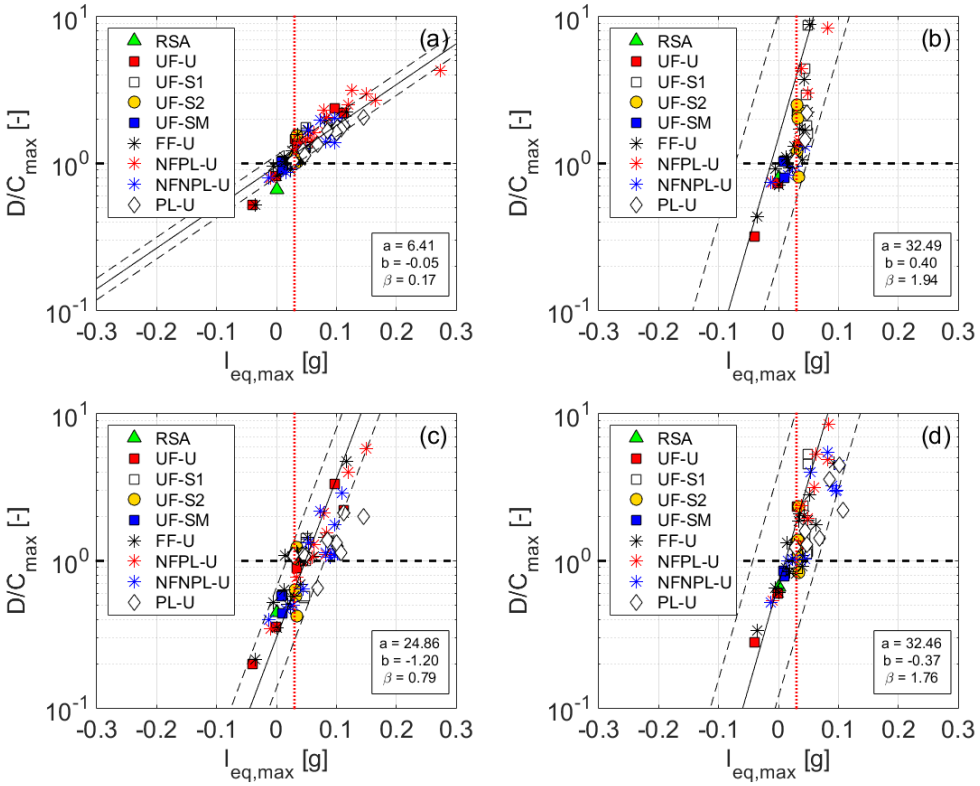

Figure 9 Linear regression (black line) in the $\log(D/C)_{max}$ vs $I_{eq,max}$ space, ±σ confidence bands (black dashed lines) and optimal value of I_{eq} (red dashed line) for different group of structural members: (a) floor beams, (b) staircase beams, (c) columns, and (d) squat columns.

5.2.1 Fitting of the results with $I_{eq,SRSS}$

In this section, a linear regression of the results in the semi-logarithm space of the maximum flexural *D/C* ratio versus the maximum ground motion index $I_{eq,SRSS}$ for each earthquake (i.e., $\log(D/C)_{max}$ vs $I_{eq,SRSS,max}$) and its confidence bands are obtained in order to show the differences with respect to I_{eq} and to justify which index is more suitable for identifying possible unacceptable cases for LTHA design. Results obtained by relating $I_{eq,SRSS}$ (see Equation (4)) to the *D/C* ratio of each earthquake within the selected ground motion suites are presented in Figure 10. Linear regressions of the results show values of R^2 equal to 0.53, 0.38, 0.53 and 0.31 for floor beams, staircase beams, squat columns and other columns, respectively. These values are lower than the case with I_{eq}, showing that for the purpose of this paper I_{eq} is a better candidate compared to $I_{eq,SRSS}$.

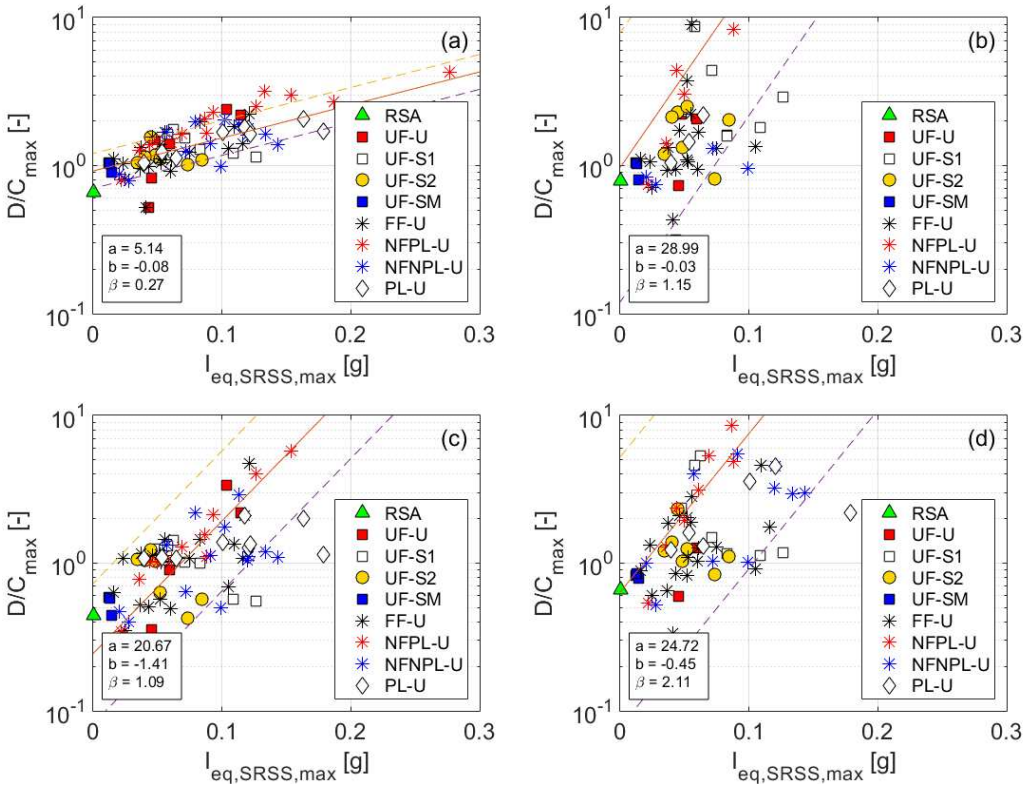

Figure 10 Linear regression (black line) in the $\log(D/C)_{max}$ vs $I_{eq,SRSS,max}$ space, $\pm\sigma$ confidence bands (black dashed lines) for different group of structural members: (a) floor beams, (b) staircase beams, (c) columns, and (d) squat columns.

6. CONCLUSIONS

The scope of this work is to contribute to the diffusion of Linear Time-History Analysis (LTHA) as a practicable seismic design method of analysis. In particular, a clear and complete framework for EC8-compliant LTHA design of Reinforced-Concrete (RC) Moment-Resisting-Frame (MRF) buildings is presented and it is meant to contribute in enlarging the availability of practical examples on this topic in literature.

Even if the theoretical principle of LTHA is well known to every engineer (solution of the equations of motion for linear-elastic multi-degree of freedom systems), the lack of a clear and detailed design framework makes LTHA not easy to be utilised by designers, especially with regard to the input selection. For the first time, ASCE/SEI 7-16 includes LTHA among the possible seismic design methods with clear indications on how to employ it for design of structures. In these standards, the suggested input selection method is spectral-matching with the intent to have results similar to the Response Spectrum Method (RSA) avoiding the problem of modal combination and keeping the correlation between local force components. In this paper,

a new procedure to implement LTHA for design purposes according to EC8 has been presented and discussed at each step (i.e., ground motion selection, modelling, behaviour factor, damping model, P-Delta effects, load combinations, verifications, and results interpretation). In particular, the possibility of using the spectrum-compatibility procedure provided by Eurocode 8 for Nonlinear Time-History Analysis (NTHA) has been investigated herein. This can be very relevant as if the ground motion selection procedure is perfectly compatible with NTHA, it allows a direct comparison between linear and nonlinear results using the same suite of ground motions. This direct linear-nonlinear comparison is not achievable if conventional RSA design is performed or the spectral-matching suggested by FEMA P-1050 and ASCE/SEI 7-16 is considered.

In order to provide a simple tool for designers approaching ground motion selection for LTHA, this paper presents an index which is building-dependent and allows to identify, at preliminary stage, potential unacceptable responses for LTHA at ultimate limit states. Unacceptable responses can make LTHA design particularly problematic when evaluating capacities of RC members according to "force-based" approaches, resulting in disproportionally high demand/capacity ratios and expensive solutions. Moreover, this index, used together with specific criteria that can be identified by designers, allows to account for record-to-record variability in LTHA results.

Results have been obtained for a regular 12-storey RC-MRF as an example, but they can be considered as a benchmark for designers approaching LTHA design. The benchmark building herein analysed accounts for critical aspects, such a quite large number of storeys for frames, the presence of a staircase and squat columns, high concrete class for ordinary use, and different field-specific conditions referred to fault. For this reason, the results obtained from this study can be considered as a reasonable reference for ordinary buildings.

It has been shown that LTHA represents a seismic design method which avoids the approximations of other linear seismic analysis methods, leads to conservative results and can be applied to any structure (e.g., irregular buildings). However, further investigations are needed to show quantitatively the applicability of the procedure in the case of irregular buildings including accidental eccentricity, but, in analogy with other analysis procedures, there is no specific reason why it should not be suitable for irregular buildings. Finally, LTHA can be used for design of buildings in seismic areas prone to near-field conditions (e.g., pulse-like) as herein shown, but further investigations on this aspect are needed.

ACKNOWLEDGMENTS

The first author is thankful for the support received by the University of Bristol Alumni foundation. This research is funded by the Leverhulme Trust (RPG-2017-006, GENESIS project) for the second author. The authors are grateful to the two anonymous reviewers for their useful comments.

REFERENCES

[1] European Committee for Standardization (CEN). Eurocode 8: Design of structures for earthquake resistance – Part 1: General rules, seismic actions and rules for buildings, EN 1998-1:2004, Brussels, BE; 2004a.

[2] American Society of Civil Engineers (ASCE). Minimum design loads and associated criteria for buildings and other structures, ASCE/SEI 7-16, Reston, VA; 2017

[3] Mwafi AM and Elnashai A. Overstrength and force reduction factors of multistorey reinforced-concrete buildings. Structural Design of Tall Buildings 2002; 11(5):329-351.

[4] Chopra AK. Dynamics of the structures: theory and applications to earthquake engineering. Pearson, 4th Edition, Prentice Hall; 2012.

[5] Standards New Zealand. Structural design actions – Part 5: Earthquake actions, NZS 1170.5:2004, Wellington, NZ; 2004.

[6] Italian Building Code 2018. Technical recommendations for buildings – D.M. 17/01/2018. G.U. n.42 del 20/02/2018. Rome, Italy; 2018 (in Italian)

[7] Der Kiureghian A. A response spectrum method for random vibration analysis of MDF systems. Earthquake Engineering and Structural Dynamics 1981; 9:419-435.

[8] Gupta AK. Response spectrum method in seismic analysis and design of structures. CRC Press; 1992.

[9] Cacciola P, Colajanni P, and Muscolino G. Combination of modal responses consistent with seismic input representation. Journal of Structural Engineering, ASCE, 2004; 130:47-55.
[10] De Luca F and Verderame GM. The accuracy of CQC and response spectrum analysis in the case of impulsive earthquakes. Proceedings of the 11th International Conference on Structural Safety and Reliability, ICOSSAR 2013.
[11] Wilson E. Termination of the response spectrum method, 2015. Available at: https://ryanrakhmats.wordpress.com/2015/11/27/ed-wilson-termination-of-the-response-spectrum-method/. Last access in July 2018.
[12] Charney F. A new linear response history analysis procedure for the 2015 NEHRP Recommended Provisions and for ASCE 7-16. Structural Congress 2015.
[13] De Luca F and Lombardi L. EC8 Design through Linear Time-History Analysis versus Response Spectrum Analysis – Is It an Enhancement for PBEE? Proceedings of the 16th World Conference on Earthquake Engineering, WCEE, 2017.
[14] Taghavi S and Miranda E. Response of non-structural building elements, PEER Report 2003/05, Pacific Earthquake Engineering Research Center; 2003.
[15] Ghanaat Y. Failure modes approach to safety evaluation of dams. Proceedings of the 13th World Conference on Earthquake Engineering, WCEE, 2004.
[16] Yamaguchi Y, Hall R, Sasaki T, Matheu E, Kanenawa K, Chudgar A, and Yule D. Seismic performance evaluation of concrete gravity dams. Proceedings of the 13th World Conference on Earthquake Engineering, WCEE, 2004.
[17] Nour A, Cherfaoui A, Gocevski V, and Leger P. CANDU 6 nuclear power plant: reactor building floor response spectra considering seismic wave incoherency. Proceedings of the 15th World Conference on Earthquake Engineering, WCEE, 2012.
[18] McGuire RK. Seismic hazard and risk analysis (MNO-10), Earthquake Engineering Research Institute (EERI), 1st Edition; 2004.
[19] Tothong P, Cornell A, and Baker JW. Explicit directivity-pulse inclusion in probabilistic seismic hazard analysis. Earthquake Spectra 2007; 23(4):867-891.
[20] Iervolino I, De Luca F, and Cosenza E. Spectral shape-based assessment of SDOF nonlinear response to real, adjusted and artificial accelerograms. Engineering Structures 2010a; 33:2776-2792.
[21] Baker JW. Conditional mean spectrum: tool for ground-motion selection. Journal of Structural Engineering, ASCE, 2011; 137(3):322-331.
[22] American Society of Civil Engineers (ASCE). Minimum design loads and associated criteria for buildings and other structures, ASCE/SEI 7-02, Reston, VA; 2003
[23] Building Seismic Safety Council (BSSC). 2015 NEHRP Recommended Seismic Provisions for New Buildings and Other Structures, FEMA P-1050, Washington, DC; 2015
[24] Whittaker A, Atkinson G, Baker J, Bray J, Grant D, Hamburger R, Haselton C, and Somerville P. Selecting and scaling earthquake ground motions for performing response-history analyses, NIST GCR 11-917-15, prepared for the National Institute of Standards and Technology by the NEHRP Consultants Join Venture, Gaithersburg, MD; 2011.
[25] Chioccarelli E and Iervolino I. Near-source seismic demand and pulse-like records: a discussion for L'Aquila earthquake. Earthquake Engineering and Structural Dynamics 2010; 39:1039-1062.
[26] Aswegan K and Charney FA. A simple linear response history analysis procedure for building codes. Proceedings of the 10th US National Conference in Earthquake Engineering, 2014.
[27] Building Seismic Safety Council (BSSC). 2015 NEHRP Recommended Seismic Provisions: Design Examples. FEMA P-1051, Washington, DC, 2016.
[28] Pacific Earthquake Engineering Research Center (PEER), PEER NGA Ground Motion Database, 2014. Available at: https://ngawest2.berkeley.edu/site. Last access in July 2018.
[29] European Strong-Motion database (ESM), EC Commission for Community Research 5th Framework, 2008. Available at: http://www.isesd.hi.is/ESD_Local/frameset.htm. Last access in July 2018
[30] Cornell CA. Hazard, ground motions and probabilistic assessment for PBSD, PEER report 2004/05, Pacific Earthquake Engineering Research Center; 2004.
[31] Luco N, Ellingwood BR, Hanburger RO, Hooper JD, Kimball JK, and Kircher CA. Risk-targeted versus current seismic design maps for the conterminous United States. Proceedings of the 76th Annual SEAOC Convention, SEAOC, 2007.

[32] Calvi G. M. Revisiting design earthquake spectra. Earthquake Engineering & Structural Dynamics 2018; https://doi.org/10.1002/eqe.3101
[33] Bommer JJ, Scott SG, and Sarma SK. Hazard-consistent earthquake scenario. Soil Dynamics and Earthquake Engineering 2000; 19(4):219-231.
[34] Jayaram N, Lin T, and Baker JW. A Computationally Efficient Ground-Motion Selection Algorithm for Matching a Target Response Spectrum Mean and Variance. Earthquake Spectra 2011; 27(3):797-815.
[35] Goda K and Atkinson GM. Seismic performance of wood-frame houses in south-western British Columbia. Earthquake Engineering and Structural Dynamics 2011; 40:903-924.
[36] Iervolino I, Galasso C, and Cosenza E. REXEL: computer aided record selection for code-based seismic structural analysis. Bulletin of Earthquake Engineering 2010b; 8:339-362.
[37] Cimellaro GP and Marasco S. A computer-based environment for processing and selection of seismic ground motion records: OPENSIGNAL. Frontiers in Built Environment 2015; 1(17):1-13.
[38] Jayamon JR and Charney F. Multiple ground motion response spectrum match tool for use in response history analysis. Structural Congress 2015.
[39] Tothong P and Luco N. Probabilistic seismic demand analysis using advanced ground motion intensity measures. Earthquake Engineering and Structural Dynamics 2007; 36(13):1837-1860.
[40] Kottke A and Rathje EM. A Semi-Automated Procedure for Selecting and Scaling Recorded Earthquake Motions for Dynamic Analysis. Earthquake Spectra 2008; 24(4):911-932.
[41] Katsanos EI, Sextos AG and Manolis GD. Selection of earthquake ground motion records: A state-of-the-art review from a structural engineering perspective. Soil Dynamics and Earthquake Engineering 2010; 30(4):157-169.
[42] Hancock J, Watson-Lamprey J, Abrahamson NA, Bommer JJ, Markatis A, Mccoy E, and Mendis R. An improved method of matching response spectra of recorded earthquake ground motion using wavelets. Journal of Earthquake Engineering 2006; 10(1):67-89.
[43] Meletti C, Meroni F, Martinelli F, Locati M, Cassera A, and Stucchi M. Ampliamento del sito web per la disseminazione dei dati del progetto S1. 2007. Available at: http://esse1.mi.ingv.it/. Last access in July 2018.
[44] Woessner J, Laurentiu D, Giardini D, Crowley H, Cotton F, Grunthal G, Valensise G, Arvdsson R, Basili R, Demircioglu MB, Hiemer S, Meletti C, Musson RW, Rovida AN, Sesetyan K, Stucchi M., and the SHARE Consortium. The 2013 European Seismic Hazard Model: key components and results. Bulletin of Earthquake Engineering 2015; 13:3553-3596. http://www.shareeu.org/
[45] Almufti I, Motamed R, Grant DN, and Willford M. Incorporation of velocity pulses in design ground motions for response history analysis using a probabilistic framework. Earthquake Spectra 2015; 31(3):1647-1666.
[46] Kohrangi M, Vamvatsikos D, and Bazzurro P. Pulse-like versus non-pulse-like ground motion records: Spectral shape comparisons and record selection strategies. Earthquake Engineering and Structural Dynamics 2018; 1-19.
[47] Somerville PG, Smith NF, Graves RW, and Abrahamson NA. Modification of empirical strong ground motion attenuation relations to include the amplitude and duration effects of rupture directivity. Seismological Research Letters 1997; 68(1):199-222.
[48] Abrahamson NA. Effects of rupture directivity on probabilistic seismic hazard analysis. Sixth International Conference on Seismic Zonation, 2000.
[49] Akkar S, Yazgan U, and Gulkan P. Drift estimates in frame buildings subjected to near-fault ground motions. Journal of Structural Engineering 2005; 131(7):1014-1024.
[50] Luco N and Cornell CA. Structure-specific scalar intensity measures for near-source and ordinary earthquake ground motions. Earthquake Spectra 2007; 23(2):357-392.
[51] Applied Technology Council. Quantification of building seismic performance factors, FEMA P-695, prepared for the Federal Emercency Management Agency, Washington, DC; 2009.
[52] Baker JW. Quantitative classification of Near-Fault ground motions using wavelet analysis. Bulletin of the Seismological Society of America 2007; 97(5):1486-1501.
[53] Campbell K and Bozorgnia Y. Campbell-Bozorgnia NGA Ground Motion Relations for the Geometric Mean Horizontal Component of Peak and Spectral Ground Motion Parameters. PEER Report No. 2007/02, Pacific Earthquake Engineering Research Center, University of California, Berkeley, 2007.
[54] Watson-Lamprey J and Boore DM. Beyond SaGMRotI: Conversion to SaArb, SaSN, and SaMaxRot. Bulletin of the Seimological Society of America 2007; 97(5):1511-1524.

[55] Stewart JP, Abrahamson NA, Atkinson GM, Baker JW, Boore DM, Bozorgnia Y, Campbell KW, Comartin CD, Idriss IM, Lew M, Mehrain M, Moehle JP, Naeim F, and Sabol TA. Representation of bidirectional ground motions for design spectra in building codes. Earthquake Spectra 2011; 27(3):927-937.
[56] Shahi SK. A probabilistic framework to include the effects of near-fault directivity in seismic hazard assessment, a dissertation for the degree of PhD, Stanford University; 2013.
[57] European Committee for Standardization (CEN). Eurocode 2: Design of concrete structures – Part 1-1: General rules and rules for buildings, EN 1992-1-1:2004, Brussels, BE; 2004b.
[58] Akinci A, Galadini F, Pantosti D, Petersen M, Malagnini L, and Perkins D. Effect of time dependence on probabilistic seismic-hazard maps and deaggregation for the Central Apennines, Italy. Bulletin of the Seismological Society of America 2009; 99(2A):585-610.
[59] Open Systems for Earthquake Engineering Simulation, OpenSees. Pacific Earthquake Engineering Center (PEER), 2006. Available at: http://opensees.berkeley.edu/. Last download is OpenSees v2.5.0 in September 2017.
[60] Young WC and Budynas RG. Roark's formulas for stress and strain, 7th Edition, McGraw-Hill; 2002.
[61] Fardis MN. Seismic design, assessment and retrofitting of concrete buildings – based on EN-Eurocode 8. Springer; 2009.
[62] Kappos AJ. Evaluation of behaviour factors on the basis of ductility and overstrength studies. Engineering Structures 1999; 21:823-835.
[63] Elnashai AS and Mwafy AM. Overstrength and force reduction factors of multistorey reinforced-concrete buildings. The Structural Design of Tall Buildings 2002; 11:329-351.
[64] Chopra AK and McKenna F. Modelling Viscous Damping in Nonlinear Response History Analysis of Buildings for Earthquake Excitation. Earthquake Engineering and Structural Dynamics 2016; 45:193-211.
[65] Giannopoulos D., & Vamvatsikos D. Ground motion records for seismic performance assessment: To rotate or not to rotate? Earthquake Engineering & Structural Dynamics 2018; 47:2410-2425.
[66] De La Llera JC and Chopra AK. Accidental torsion in buildings due to base rotational excitation. Earthquake Engineering and Structural Dynamics 1994; 23:1003:1021.
[67] Basu D, Constantinou MC, and Whittaker A. An equivalent accidental eccentricity to account for the effects of torsional ground motion on structures. Engineering Structures 2014; 69:1-11.
[68] Mander JB, Priestley MJN, and Park R. Theoretical stress-strain model for confined concrete. Journal of Structural Engineering, ASCE, 1988; 114(8):1804-1826.
[69] Menegotto M and Pinto PE. Method of analysis for cyclically loaded RC frames including changes in geometry and non-elastic behaviour of elements under combined normal force and bending. Report N.32, University of Rome; 1972.
[70] Shome N and Cornell CA. Probabilistic seismic demand analysis of nonlinear structures. Report RMS-35, RMS Program, Stanford University, Stanford, California, 1999.
[71] Luco N and Bazzurro P. Does amplitude scaling of ground motion records result in biased nonlinear structural drift responses? Earthquake Engineering and Structural Dynamics 2007; 36:1813-1835.